

University of New Hampshire

University of New Hampshire Scholars' Repository

Master's Theses and Capstones

Student Scholarship

Winter 2019

Tree Species Traits Determine the Success of LiDAR-based Crown Mapping in a Mixed Temperate Forest

John Hastings

University of New Hampshire, Durham

Follow this and additional works at: <https://scholars.unh.edu/thesis>

Recommended Citation

Hastings, John, "Tree Species Traits Determine the Success of LiDAR-based Crown Mapping in a Mixed Temperate Forest" (2019). *Master's Theses and Capstones*. 1326.

<https://scholars.unh.edu/thesis/1326>

This Thesis is brought to you for free and open access by the Student Scholarship at University of New Hampshire Scholars' Repository. It has been accepted for inclusion in Master's Theses and Capstones by an authorized administrator of University of New Hampshire Scholars' Repository. For more information, please contact nicole.hentz@unh.edu.

Tree Species Traits Determine the Success of LiDAR-based Crown Mapping in a Mixed Temperate Forest

BY

JACK HASTINGS

BS, University of New Hampshire, 2016

THESIS

Submitted to the University of New Hampshire

In Partial Fulfillment of

the Requirements for the Degree of

Master of Science

in

Natural Resources

December 2019

This thesis was examined and approved in partial fulfillment of the requirements for the degree of Master of Science in Natural Resources by:

Dr. Scott V. Ollinger, Thesis Director
Professor of Natural Resources
University of New Hampshire

Dr. Michael W. Palace
Associate Research Professor, Earth Sciences
University of New Hampshire

Dr. Mark J. Ducey
Professor of Natural Resources
University of New Hampshire

On August 23, 2019

Approval signatures are on file with the University of New Hampshire Graduate School

Table of Contents

Table of Contents	iii
List of Tables	iv
List of Figures	v
Abstract	vii
Introduction.....	1
Methods.....	3
Site Description.....	3
Remote Sensing Data.....	4
Crown Delineation	5
Parameter Tuning and Accuracy Assessment.....	8
Statistical Analysis.....	10
Results.....	12
Manual Crown and Plot Characteristics	12
Automated Crown Delineation Accuracy	14
Differences in methods and influence of parameter tuning	14
Overall and plot-level accuracy	14
Differences in accuracy across species	15
Variables Influencing Accurate Automated Crown Delineation	16
Linear regressions	16
Logistic Regressions	17
Discussion.....	19
Tree Architecture	19
Tree size	19
Crown Spread.....	21
Mechanical interaction.....	23
A traits perspective	24
Species Evenness	26
A silver lining: where do these methods work?.....	27
Moving forward	28
Conclusion	29
Supplemental Material	31

List of References 38

List of Tables

Table 1: Five automated LiDAR-based individual tree crown delineation routines were evaluated in this study. †Four routines are surface-based methods applied to rasterized canopy height models. ‡The fifth routine is a 3D method applied to a point cloud. All routines were implemented in the R package lidR, developed by Roussel and Auty (2019). 7

Table 2: Overall site accuracy (%) of five different automated crown delineation techniques. The table included default, generalized, and plot-tuned parameters. † Conifer and hardwood accuracies are from plot-tuned model runs. 15

Table 3: Results of the logit models assessing the important tree- and plot-level variables influencing the odds of successful individual tree crown delineation. All variables were standardized prior to analyses. The table includes the 10-fold cross-validation (CV %) model accuracy estimates, coefficients of variables in the models and the corresponding standard error (SE) (*p <0.05, **p < 0.01, ***p < 0.001)..... 18

Table 4: Results from multivariate models assessing the influence of plot-level metrics on overall accuracy of five automated crown delineation methods. The table includes the coefficients of variables in the models and the corresponding standard error (SE) (*p <0.05, **p < 0.01, ***p < 0.001)..... 32

Table 5: Results from accuracy assessment from five different automated crown delineation method at the plot level. The table includes plot-tuned, generalized, and default parameter accuracy. 34

List of Figures

- Figure 1:** This study was conducted in a ForestGEO MegaPlot (outlined in red) in the Prospect Hill Tract (inset) of the Harvard Forest, in Petersham, Massachusetts, USA. 4
- Figure 2:** Manual crown delineation was performed using high resolution UAV imagery. All delineations were done on the September 13th image (left panel), but other dates of imagery were used to help differentiate crowns growing in close proximity. The right panel (October 12th) gives an example of phenologic differences between species that can be leveraged to help separate crowns that might otherwise be clumped during manual interpretation..... 6
- Figure 3:** Automated crown delineations (A_{ITC} ; shown with bold outline) were assessed against manual crown delineations (M_{ITC} ; shown with green fill) and assigned into one of four categories based on overlapping area: **a) Over-segmentation:** The intersecting area between A_{ITC} and M_{ITC} is greater than or equal to 50% of the area of only A_{ITC} . **b) True Positive:** The intersecting area between A_{ITC} and M_{ITC} is greater than or equal to 50% of the area of both A_{ITC} and M_{ITC} 10
- Figure 4:** Density distribution of tree-level variables showing differences between conifer and hardwood functional groups. Conifers tend to have high diameter at breast height (DBH) and crown height values, while hardwoods tend to have larger crown area values. 13
- Figure 5:** All automated crown delineation methods showed similar species level accuracy. Generally, conifer species (eastern hemlock, red pine, white pine and spruce) were more accurately delineated than hardwood species. 16
- Figure 6:** Linear regression analysis for plot-level variables and accuracy of one of the automated crown delineation methods (DALPONTE). Points are colored to show how each relationship is co-related to the fraction of conifer crown area per plot (conifer fraction). The relationship between accuracy and evenness (J) was significant ($p < 0.05$) across all methods. However, the relationship between accuracy and aggregation index (AGI) was only significant for DALPONTE AND SILVA, and the relationship between accuracy and rumple index was only significant for DALPONTE, SIVLA and LI. 17
- Figure 7:** G-LiHT LiDAR point cloud comparison highlighting the differences in structure between a hardwood dominated stand (A) and a conifer dominated stand (B). Warmer colors represent higher points in the canopy. The conifer dominated stand exhibits higher canopy rumple, and uniformity of crown shape. The conical, less-plastic shape of conifer crowns may also reduce canopy space filling efficiency. 20
- Figure 8:** Two-dimensional density plot showing different patterns of crown delineation accuracy between conifer and hardwood functional groups. The circles provide crown size comparison for two end member species: red pine (shown in red circles) and red oak (shown in blue circles). This figure corresponds with delineation categories described in Figure 3: the top right quadrant signifies true delineations, the top left signifies over-segmentation, the bottom

right signifies under-segmentation, and the bottom left signifies false positive. This figure shows data generated from the DALPONTE method, though all methods show similar patterns..... 22

Figure 9: Relationships between the fraction of conifer crown area per plot (conifer fraction) and Shannon’s Diversity Index (A), Rumple Index (B), Pielou’s Evenness Index (C), trees per plot (D), and Aggregation Index (E). 31

Figure 10: Following parameter tuning, plot-level accuracy varied similarly by methods across plot, indicating that accuracy is largely controlled by the structure and composition of the plots rather than methodological differences. 32

Figure 11: September UAV image collected over the MegaPlot showing the location of the fifteen plots used in this study. 33

Figure 12: UAV imagery collected over the ForestGEO MegaPlot on September 13th (A), October 12th (B), October 22th (C) and November 4th (D). All these dates of imagery were used to during manual crown delineation interpretation. The images highlight differences in phenology that may be useful for future crown delineation work. 35

Figure 13: Emergent white pine crowns stand out as hotspots on a canopy height model. Low density wood allows white pine to grow taller than all other species in the Harvard Forest. They can often stand five or more meters above the continuous canopy. 36

Figure 14: Red pine often exhibit crown shyness when grown in monoculture. Panel A shows crown shyness from below the canopy, while Panel B shows it from above the canopy..... 36

Figure 15: Conifer and hardwood functional groups show distinct differences in foliar nitrogen and wood density (specific gravity) that influence overall tree architecture and how they interact with neighboring crowns. There is also considerable variation of traits within functional groups. Average foliar %N values taken from Northeastern Ecosystem Research Cooperative (2010). Average specific gravity values taken from Ducey and Knapp (2010). 37

Acknowledgement

Foremost, I would like to express my gratitude to my committee members, Dr. Scott Ollinger, Dr. Mark Ducey, and Dr. Michael Palace. Without their guidance, support, and insight this thesis would have been a very different and less impactful document. Thank you for giving me near complete freedom to choose my thesis direction, and for not batting an eye at the sinuous path it has taken.

I would like to especially thank my advisor, Dr. Scott Ollinger, for responding to my email inquiry for undergraduate research experiences back in the winter of 2014. I did not know it at the time but joining the Terrestrial Ecosystem Analysis Lab was one of the best opportunities I have had. I sincerely believe that I have learned more and made more true connections – both academic and lifelong friendships – during my years with TEAL than anywhere else during my academic journey. I also would like to thank Scott for providing me with a template for how to have an impactful scientific career while still pursuing all the other passions in life. Thank you for accepting me as a student even after I ran away multiple times to go on adventures of my own. Who knows, maybe I'll be back again one day.

I would like to thank all past and present members of TEAL that I have had the pleasure to do field and lab work with throughout the years. While I always take pleasure in the solitude of being in the woods alone, field work was undoubtedly always made better by their banter and witticism, especially when hauling 50lbs of gear up to the 10T plot at Bartlett. Nowhere else could I find a group of people that would allow me to climb 100 ft towers or shoot shotguns, and somehow learn a whole lot in the process.

I would like to highlight Lucie Lepine, especially. Lucie put unwavering faith in my fieldwork ability and allowed me to assume responsibilities within TEAL that pushed me to grow both as a scientist and as human. She has been a true friend, and a remote sensing guru for me to turn to when I was perplexed.

Thank you to Dr. Rebecca Sanders-DeMott and Frankie Sullivan. Both Rebecca and Frankie have been early career scientist role models for me. Their willingness to share knowledge, skills, and insight has been an invaluable resource to me during this thesis. Thank you to Frankie for helping me get running with R scripting – it turns out I really enjoy writing lines of code. Thank you to Rebecca for her master-craft wordsmithing – her edits and revisions have helped turn my bearish writing into something far more eloquent.

Thank you to Dr. Andrew Ouimette. Andy allowed me to steal countless hours of his time to discuss my thesis (and any number of tangential hair-brain ideas). His insight has been invaluable from the genesis of my thesis, and he should be given substantial credit for helping me shape this research project. We all know the final product is a near unrecognizable creature to what it started as – and I think all the better for it. I really believe a large part of the reason this thesis was so successful was because I was able to share an office with Andy (and Rebecca). I had complete freedom to openly discuss my own ideas, but I was also included as an equal in other academic discussions. Beyond being a mentor, Andy has also been a great friend – one

who was just as willing to share a meal as to help fix a car – and I value his friendship far beyond his academic mentorship.

Thank you to my expanding family – Hastings and Langley. It's a blessing that they get along so well and continue to do things together even though Kate and I are now on the other side of the country. Mom and Dad, thank you for absolutely everything you've done to get me to this point. Tina and John, thank you for welcoming me into your family.

And of course, most of all thank you to my amazing partner, Kate. I've said it before but isn't it funny how I had to go halfway around the world to find out that my Love was living so close by for so long and I didn't know it? On to our next adventure.

Oh, and I guess I should officially dedicate my thesis to my dog, Indiana. How else would I have found so much extra time to walk in the woods? Every day you remind me that you really are a dog...

Abstract

Tree Species Traits Determine the Success of LiDAR-based Crown Mapping in a Mixed Temperate Forest

by

Jack Hastings

Department of Natural Resources, University of New Hampshire

Automated individual tree crown delineation (ITCD) via remote sensing platforms offers a path forward to obtain wall-to-wall detailed tree inventory/information over large areas. While LiDAR-based ITCD methods have proven successful in conifer dominated forests, it remains unclear how well these methods can be applied broadly in deciduous broadleaf (hardwood) dominated forests. In this study, I applied five common automated LiDAR-based ITCD methods across fifteen plots ranging from conifer- to hardwood- dominated at the Harvard Forest in Petersham, MA, USA, and assess accuracy against manually delineation crowns. I then identified basic tree- and plot-level factors influencing the success of delineation techniques. My results showed that automated crown delineation shows promise in closed canopy mixed-species forests. There was relatively little difference between crown delineation methods (51-59% aggregated plot accuracy), and despite parameter tuning, none of the methods produce high accuracy across all plots (27 – 90% range in plot-level accuracy). I found that all methods delineate conifer species (mean 64%) better than hardwood species (mean 42%), and that accuracy of each method varied similarly across plots and was significantly related to plot-level conifer fraction.

Further, while tree-level factors related to tree size (DBH, height and crown area) all strongly influenced the success of crown delineations, the influence of plot-level factors varied. Species evenness (relative species abundance) was the most important plot-level variable controlling crown delineation success, and as species evenness decreased, the probability of successful delineation increased. Evenness was likely important due to 1) its negative relationship to conifer fraction and 2) a relationship between evenness and increased canopy space filling efficiency. Overall, my work suggests that the ability to delineate crowns is not strongly driven by methodological differences, but instead driven by differences in functional group (conifer vs. hardwood) tree size and diversity and how crowns are displayed in relation to each other. While LiDAR-based ITCD methods are well suited for conifer dominated plots with distinct canopy structure, they remain less reliable in hardwood dominated plots. I suggest that future work focus on integrating phenology and spectral characteristics with existing LiDAR approaches to better delineate hardwood dominated stands.

Introduction

Individual tree crown delineation (ITCD) via remote sensing platforms offers a path forward to obtain wall-to-wall detailed tree inventory/information over large areas. ITCD has been used to map species (Shi et al., 2018), biodiversity (Zhao et al., 2018), and carbon stocks (Coomes et al., 2017), as well as to quantify tree structural (Palace et al., 2008) and spectral characteristics (Clark et al., 2005). While manually delineating crowns from high resolution imagery provides accurate measurements for small scale studies (Asner et al., 2002; Clark et al., 2005; Fang et al., 2018), effective automated methods are necessary if efforts are to be scaled to larger geographic regions. An ideal crown delineation method would be broadly applicable across stands varying in structural and compositional complexity. Given that many forests across the globe are under increasing pressure from climate change (Rustad et al., 2012), invasive pests (Crowley et al., 2016), and land-use change (Houghton, 1995), reliable methods for measuring and mapping forests takes on additional urgency. Despite this need, broad-scale application of automated ITCD techniques remains difficult and unreliability is uncertain.

Considerable work has been done to develop and improve automated ITCD techniques (Ayrey et al., 2017; Dalponte and Coomes, 2016; Jing et al., 2012; Li et al., 2012; Lu et al., 2014; Silva et al., 2016a; Wan Mohd Jaafar et al., 2018; Zhen et al., 2015). Light Detection and Ranging (LiDAR) crown delineation methods tend to be favored over spectral methods because they are not impaired by shadow and illumination artifacts (Dalponte et al., 2015), and because of the ability to directly measure crown architecture (Zhen et al., 2016). However, reported accuracies of different LiDAR-based methods is wide-ranged (Lu et al., 2014), and the success of their application is largely controlled by the structure of the forest of interest (Vauhkonen et al., 2012).

The structure of an individual crown and its position relative to neighboring crowns has a direct bearing on the success of ITCD. Crown architecture controls leaf display (Valladares and Niinemets, 2007), and trees must balance resource acquisition (e.g. light) with mechanical constraints (e.g. buckling under its own weight; Chave et al., 2009; Horn, 1971). Tree crown form is also plastic (Forrester et al., 2017; Muth and Bazzaz, 2003; Pretzsch, 2014; Valladares and Niinemets, 2007) and crown shape is a response to spatio-temporal variation in facilitative and competitive interactions with neighboring trees (Fichtner et al., 2017; Givnish, 2002), as well as a function of site history and disturbance (Forrester et al., 2017; Oliver and Stephens, 1977).

Despite the seemingly stochastic and complex nature of crown and stand structural development, there are also characteristic differences between needle-leaf evergreen (conifer) and deciduous broadleaf (hardwood) plant functional types that influence ITCD. Conifers and hardwoods exhibit differences in physiological traits and adaptation to resource acquisition, disturbance and stress (Augusto et al., 2014; Brodribb et al., 2012) that manifest in difference in crown shape and stand arrangement. LiDAR-based ITCD methods have been successfully applied in conifer dominated systems (Li et al., 2012; Silva et al., 2016b; Wang et al., 2016), while hardwood dominated systems tend to be more challenging (Broadbent et al., 2008; Zhen et al., 2016). Discrepancies in accuracy of ITCD methods between conifer and hardwood systems is often attributed to the characteristic plagiotropic growth form (ellipsoidal or umbrella-shape) of hardwood crowns that make it difficult to identify tree tops, differentiate neighboring crowns, and group split canopies of an individual crown (e.g. Lu et al. 2014).

Despite the challenges, there is a need for ITCD in many regions dominated by hardwoods and mixed stands. The temperate forests of the northeastern United States are

typically characterized by dense mixed species stands with closed canopies, where crowns often overlap and have irregular shape. Given the complexity of the forests and the dominance of hardwood trees, it remains unclear the degree to which automated ITCD techniques can be employed in the region, or what the best ITCD approach would be. Here, I applied a series of automated LiDAR-based ITCD methods across plots ranging from conifer to hardwood dominated. I identified basic tree- and plot-level factors influencing the success of delineation techniques. Finally, I comment on how the ecology of conifer and hardwoods might best be exploited to delineate trees in temperate forests.

Methods

Site Description

This study was conducted in a Smithsonian Forest Global Earth Observatory (ForestGEO) MegaPlot (Anderson-Teixeira et al., 2015) at the Harvard Forest (HF), in north-central Massachusetts (42°32' N, 72°11' W). Located within the Prospect Hill Tract of HF (**Figure 1**), the 35 ha MegaPlot is structurally and compositionally representative of the central New England landscape. It encompasses a continuous forest comprised of mature eastern hemlock (*Tsuga Canadensis*) stands, mixed-hardwood stands, remnant red pine (*Pinus resinosa*) plantations, and a 3-ha swamp (Orwig and Ellison, 2015). The age structure is dominated by 75-125 year old second growth forest (Plotkins et al., 2015). Dominant species include red oak (*Quercus rubra*), red maple (*Acer rubrum*), eastern hemlock, and white pine (*Pinus strobus*). Other common species include Norway spruce (*Picea abies*), American beech (*Fagus grandifolia*) and birch (*Betula* spp.). Between 2010 and 2014 a census of the MegaPlot was conducted, where all woody stems ≥ 1 cm were mapped, measured, and identified to species (<http://harvardforest.fas.harvard.edu:8080/exist/apps/datasets/showData.html?id=hf253>) (Orwig

and Ellison, 2015). Height of all stems were calculated using site-specific allometric equations (Sullivan et al., 2017). In 2018, I remotely established fifteen 20 m radius plots across the MegaPlot (supplemental **Figure 11**). Plots were selected to capture a full range of tree functional composition from conifer dominated to hardwood dominated.

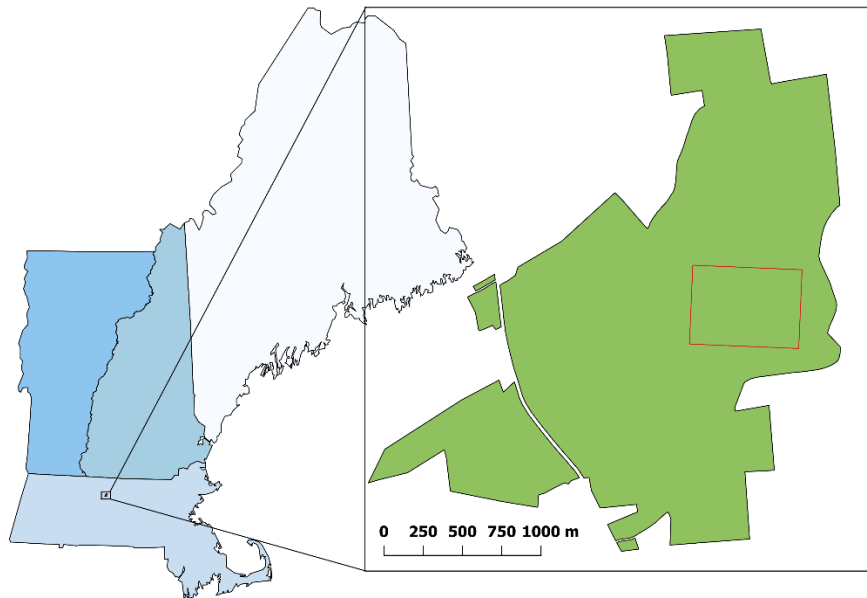


Figure 1: This study was conducted in a ForestGEO MegaPlot (outlined in red) in the Prospect Hill Tract (inset) of the Harvard Forest, in Petersham, Massachusetts, USA.

Remote Sensing Data

LiDAR and hyperspectral data were collected over Prospect Hill by NASA's Goddard LiDAR, Hyperspectral and Thermal (G-LiHT) sensor package (Cook et al., 2013) between 19-21 June, 2012. LiDAR point cloud and canopy height model (CHM), and hyperspectral data were downloaded on October 22, 2018 (<https://glihtdata.gsfc.nasa.gov/>), and clipped to a 10m buffered extent of the MegaPlot. The LiDAR point cloud has an average density of 26.98 points per m² within the MegaPlot. The hyperspectral and LiDAR CHM data have a spatial resolution of 1m.

Aerial surveys of the MegaPlot were conducted by an RGB camera-equipped unmanned aerial vehicle (UAV) throughout the 2018 growing season (David Basler, personal communication). Collected imagery had a spatial resolution of 0.01m but was down sampled to 0.1m for use in this analysis. Using the *georeferencer* plugin in QGIS (v 2.18; QGIS Development Team, 2018) UAV imagery was registered to the G-LiHT remote sensing data by identifying distinguishable features in both the UAV imagery and the hyperspectral imagery. Each UAV image was aligned with the G-LiHT imagery with 20 control points, and transformed using a first-order polynomial. The resulting georeferenced UAV images were found to be in good visual agreement and tree crowns aligned with those visible in the G-LiHT hyperspectral and LiDAR imagery and field-measured stem locations.

Crown Delineation

All tree crowns visually distinguishable within the fifteen plots were manually delineated by onscreen digitizing of the September 13th UAV image. This study excluded understory crowns not visible within UAV imagery. Manual delineation of individual tree crowns (M_{ITC}) was done with a stylus pen using the *FreehandEditing* plugin in QGIS. While crown digitization was performed on the September 13th image for consistency, multiple dates of imagery (September 13th, October 5th, October 12th, and November 4th) were used to help distinguish crowns and identify the species of each crown based on differences in shadow and phenology (*Figure 2*).

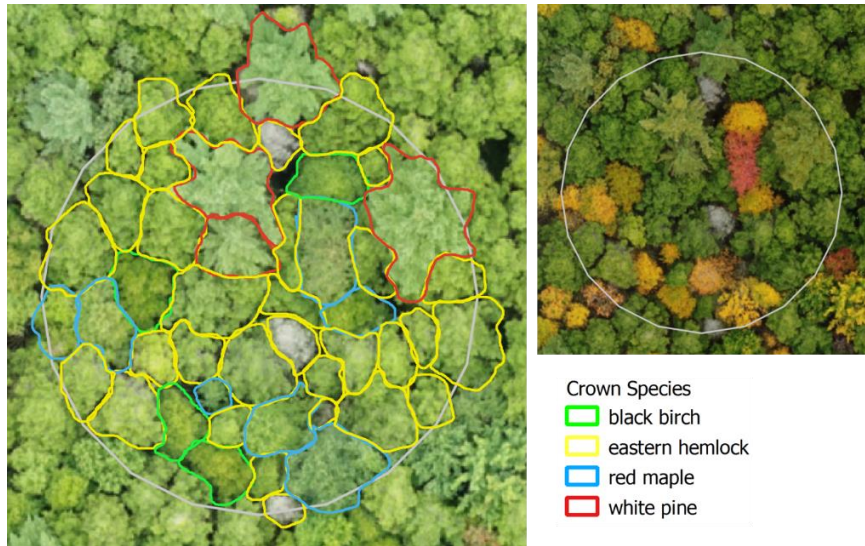


Figure 2: Manual crown delineation was performed using high resolution UAV imagery. All delineations were done on the September 13th image (left panel), but other dates of imagery were used to help differentiate crowns growing in close proximity. The right panel (October 12th) gives an example of phenologic differences between species that can be leveraged to help separate crowns that might otherwise be clumped during manual interpretation.

M_{ITC} species label and associated stem attributes (DBH and allometrically derived tree height) were assigned manually during the digitization process from the ForestGEO stem data. In rare cases where a crown could conceivably belong to one of multiple stems from either the same species or stems from different species that could not be distinguished using phenology and textural cues, the crown was assigned to the stem with the higher allometrically derived tree height. Crown area and maximum CHM-derived crown height were calculated for each M_{ITC} . Using M_{ITC} crowns, conifer fraction of each plot was calculated as the ratio of conifer crown area to hardwood crown area.

I tested five automated individual tree crown (A_{ITC}) delineation techniques (*Table 1*) available in the R (v. 3.5.1; R Core Team, 2018) package (Roussel and Auty, 2019). Four routines are surface-based methods applied to a rasterized CHM, and the fifth is a 3D method applied to a LiDAR point cloud. Dalponte2016 (DALPONTE) is a surface-based seed and region

growing method (Dalponte and Coomes, 2016). Silva2016 (SILVA) is a surface-based seed and voronoi tessellation method (Silva et al., 2016a). Simple Watershed (SWS) is an a surface-based watershed segmentation (Vincent and Soille, 1991). Marker-controlled Watershed (MCWS) is a watershed segmentation that relies on a priority seed map. Li2012 (LI) is a 3D region growing method applied to a point cloud (Li et al., 2012). All techniques were run using the *lastrees* function. Treetop priority seed points used in DALPONTE, SILVA, and MCWS were created with the *tree_detection* function using the *lmf* (local maximum filtering) algorithm (Popescu and Wynne 2013). SWS did not rely on a priority seed map, and LI has a tree top detection built into the function. While four of the five routines are surface-based methods applied to CHM, by default, all methods segment the point cloud. Final A_{ITC} polygons were generated using the *tree_hulls* function, by creating a 2D concave hull around the segmented point cloud. I chose not to smooth CHM data (e.g. Gaussian filtering) prior to crown delineation analyses. My preliminary results showed smoothing either made no marked improvement on delineation success, or, in certain cases, decreased overall accuracy of the methods.

Table 1: Five automated LiDAR-based individual tree crown delineation routines were evaluated in this study. † Four routines are surface-based methods applied to rasterized canopy height models. ‡The fifth routine is a 3D method applied to a point cloud. All routines were implemented in the R package lidR, developed by Roussel and Auty (2019).

Crown Delineation Routine	Reference
Dalponte2016 (DALPONTE)†	Dalponte and Coomes, 2016
Silva2016 (SILVA)†	Silva et al., 2016
Simple Watershed (SWS)†	Vincent and Soille, 1991
Marker-controlled Watershed (MCWS)†	Vincent and Soille, 1991
Li2012 (LI)‡	Li et al., 2012

Parameter Tuning and Accuracy Assessment

To apply each crown delineation method, we tuned parameters against manually delineated crowns. Each automated delineation technique has different input parameters controlling how the algorithm searches and delineates the CHM or point cloud, and methods vary in input parameter complexity. Parameters include search window sizes, maximum height or radius values and drop-off thresholds. I first applied each automated delineation technique with default parameters. I specified a 3x3 moving window for the *lmf* tree top detection during default parameterization because a default parameter was not given.

I then tuned each technique's input parameters to find 1) the best *plot-tuned* parameters – potentially unique parameters that maximized plot-level accuracy and 2) the best *generalized* parameters – a single set of parameters that achieved the highest accuracy when evaluated across all 15 plots. Parameter tuning was done using a bootstrapping approach, where, during each iteration, input parameters were randomly selected within a predefined range. Following each delineation iteration, accuracy was assessed by comparing the generated A_{ITC} polygons to the reference M_{ITC} delineations. Automated delineations were paired to manual delineations so that any given M_{ITC} was labeled as either correctly or incorrectly delineated. A detection accuracy score (DA) was assigned to each iteration:

$$DA = \frac{n_{TP}}{N} \quad (\text{Eq. 1})$$

where, n_{TP} is the number of correctly delineated A_{ITC} and N is the number of M_{ITC} (Yin and Wang, 2016). A given A_{ITC} was considered correctly delineated (true positive) if $\geq 50\%$ of the area of both A_{ITC} and M_{ITC} overlap (**Figure 3**; e.g. Lamar, McGraw, and Warner 2005; Leckie et al. 2004). Accuracies were recorded as plot-level accuracies, and as well as overall accuracy – aggregated across all 15 plots. Each routine except LI was iterated 500 times. LI was only

iterated 200 times because it was substantially slower than the surface-based methods and because maximum accuracy achieved did not improve beyond the first 100 iterations. I retained tuning iterations for the highest *generalized* parameter accuracy and the highest *plot-tuned* accuracy for each automated crown delineation.

To further understand how each method performed at the crown-level, I characterized the incorrect A_{ITC} delineations by type of error. Therefore, each crown was ultimately assigned one of four categories based on their overlap with M_{ITC} (**Figure 3**):

- A) Over-segmentation: The intersecting area between A_{ITC} and M_{ITC} is greater than or equal to 50% of the area of *only* A_{ITC} .
- B) True Positive: The intersecting area between A_{ITC} and M_{ITC} is greater than or equal to 50% of the area of *both* A_{ITC} and M_{ITC} (as defined above).
- C) Under-segmentation: The intersecting area between A_{ITC} and M_{ITC} is greater than or equal to 50% of the area of *only* M_{ITC} .
- D) False Positive: The intersecting area between A_{ITC} and M_{ITC} is greater than or equal to 50% of the area of *neither* A_{ITC} and M_{ITC} .

Given that any M_{ITC} can only be linked to one A_{ITC} , in the case where multiple A_{ITC} crowns fell within a single M_{ITC} (as is the case with over-segmentation), the M_{ITC} was assigned to the A_{ITC} that best overlapped with the particular M_{ITC} identified based on the A_{ITC} crown that maximized the sum of I_A and I_M , where I_A is the ratio of $A_{ITC}:M_{ITC}$ intersection area to A_{ITC} area, and I_M is the ratio of $A_{ITC}:M_{ITC}$ intersection area to M_{ITC} area.

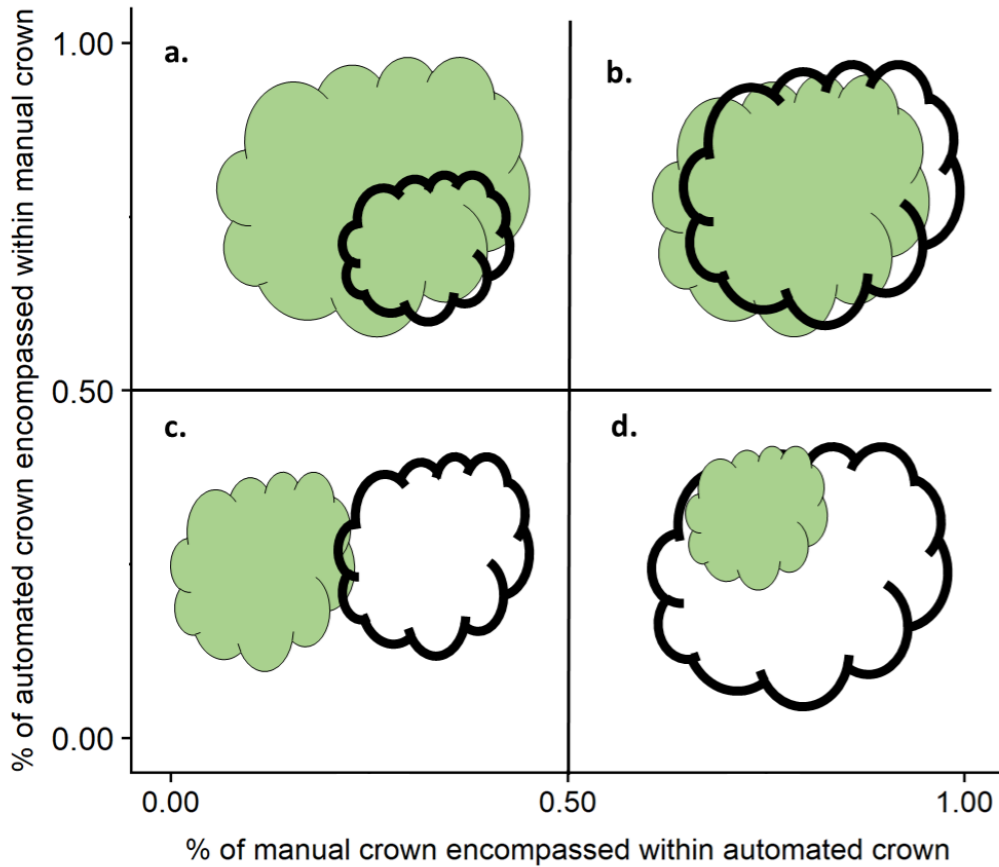


Figure 3: Automated crown delineations (A_{ITC} ; shown with bold outline) were assessed against manual crown delineations (M_{ITC} ; shown with green fill) and assigned into one of four categories based on overlapping area: **a)** Over-segmentation: The intersecting area between A_{ITC} and M_{ITC} is greater than or equal to 50% of the area of only A_{ITC} . **b)** True Positive: The intersecting area between A_{ITC} and M_{ITC} is greater than or equal to 50% of the area of both A_{ITC} and M_{ITC} . **c)** Under-segmentation: The intersecting area between A_{ITC} and M_{ITC} is greater than or equal to 50% of the area of only M_{ITC} . **d)** False Positive: The intersecting area between A_{ITC} and M_{ITC} is less than 50% of the area of both A_{ITC} and M_{ITC} .

Statistical Analysis

To understand the factors that influenced automated crown delineation I calculated multiple metrics used to describe tree-level attributes (DBH, crown height, and crown area), and plot-level vertical and horizontal structural and compositional complexity (canopy complexity, uniformity of crown spacing, relative density, trees per plot, and species diversity). Plot-level metrics only included stem attributes associated with M_{ITC} data.

Plot canopy complexity was estimated using the Rumple Index (Kane et al., 2008) – a ratio of canopy surface area to projected ground area. Uniformity of crown spacing– an aggregation index (AGI) developed by Clark and Evan (1954) – was calculated from M_{ITC} centroids as described by Pommerening (2002). Relative stem density was calculated using a mixed-species relative density equation (Ducey and Knapp, 2010). Trees per plot (TPP) was calculated as the number of M_{ITC} per plot. Species diversity was calculated using Shannon’s Diversity Index (H), Pielou’s Evenness Index (J), and species richness (Heip et al., 1998). All predictor variables were standardized to have a mean of zero and a standard deviation of one by subtracting the mean and dividing by one standard deviation (McCune and Grace, 2002).

To identify important plot-level variables I performed univariate linear regressions between all plot-level metrics and *plot-tuned* accuracy ($n = 15$) for all five crown delineation routines, and I retained any variable found to be significant ($\alpha < 5\%$) in at least one regression. I then built global multiple linear regression model including all significant variables from the univariate analyses. Multicollinearity was evaluated using variance inflation factor (VIF), and I removed highly inter-correlated variables until VIF of all variables was < 10 (Hair et al., 1995). The best model for plot-level performance was chosen using a corrected Akaike Information Criterion (AIC) to account for small sample size (Burnham and Anderson, 2002).

Finally, I built mixed-effect logistic regressions to help understand which of the tree- and plot-level factors influenced the odds that each M_{ITC} would be correctly delineated as a linear function of covariates in a logistic regression (Oberle et al., 2018). Logit models were built in the R package lme4 (Bates et al., 2015). Each global model included tree-level variables and the plot-level variables found to be significant during the univariate analyses described above. I controlled for plot-level variability by including plot as a random effect in each model. Model

selection was performed by backward elimination from the global model, and the final model was chosen by minimum AIC (Burnham and Anderson, 2002). I took the number of times a variable was included across the five models as an indication of the importance of that variable on crown delineation.

Model accuracies were evaluated using a 10-fold cross validation, where the developed logistic relationships were each trained on 90% of the data and tested on the remaining 10%. Training and testing were performed on all 10 folds of data and the results were averaged to give an estimate of each model's accuracy.

Results

Manual Crown and Plot Characteristics

I manually delineated 650 tree crowns from 14 unique species. Of those, 379 were conifer crowns, and 271 were hardwood crowns. The range in height, DBH, and crown area were comparable between conifer and hardwoods. On average conifers were taller and had larger DBH (*Figure 4*), while median conifer crown area was 27% smaller than hardwood crowns.

TPP ranged from 25 to 66 (mean 43), and structural complexity and composition varied substantially across the 15 plots. Average plot canopy height ranged from 15.5 m to 28.9 m, and average crown area ranged from 13.75 m² to 47 m². Conifer fraction, as estimated by crown area, ranged from 14% to 96%. Six of the 15 plots were characterized as conifer dominated with \geq 50% conifer fraction.

Plot level characteristics showed varying degrees of relation to conifer fraction. For example, there was a strong positive linear relationship between conifer fraction and rumple (R^2 : 0.78; $p < 0.001$). Rurple ranged from 1.34 to 2.16, with conifer dominated plots occupying the upper end of this range (1.69 – 2.16). Species evenness (J) also had a strong linear relationship

with conifer fraction (R^2 : 0.71; $p < 0.001$), as did Shannon's Index (R^2 : 0.58; $p < 0.001$). Conifer fraction showed a weak, but non-significant relationship with TPP (R^2 : 0.17; $p = 0.12$) and AGI (R^2 : 0.17; $p = 0.13$).

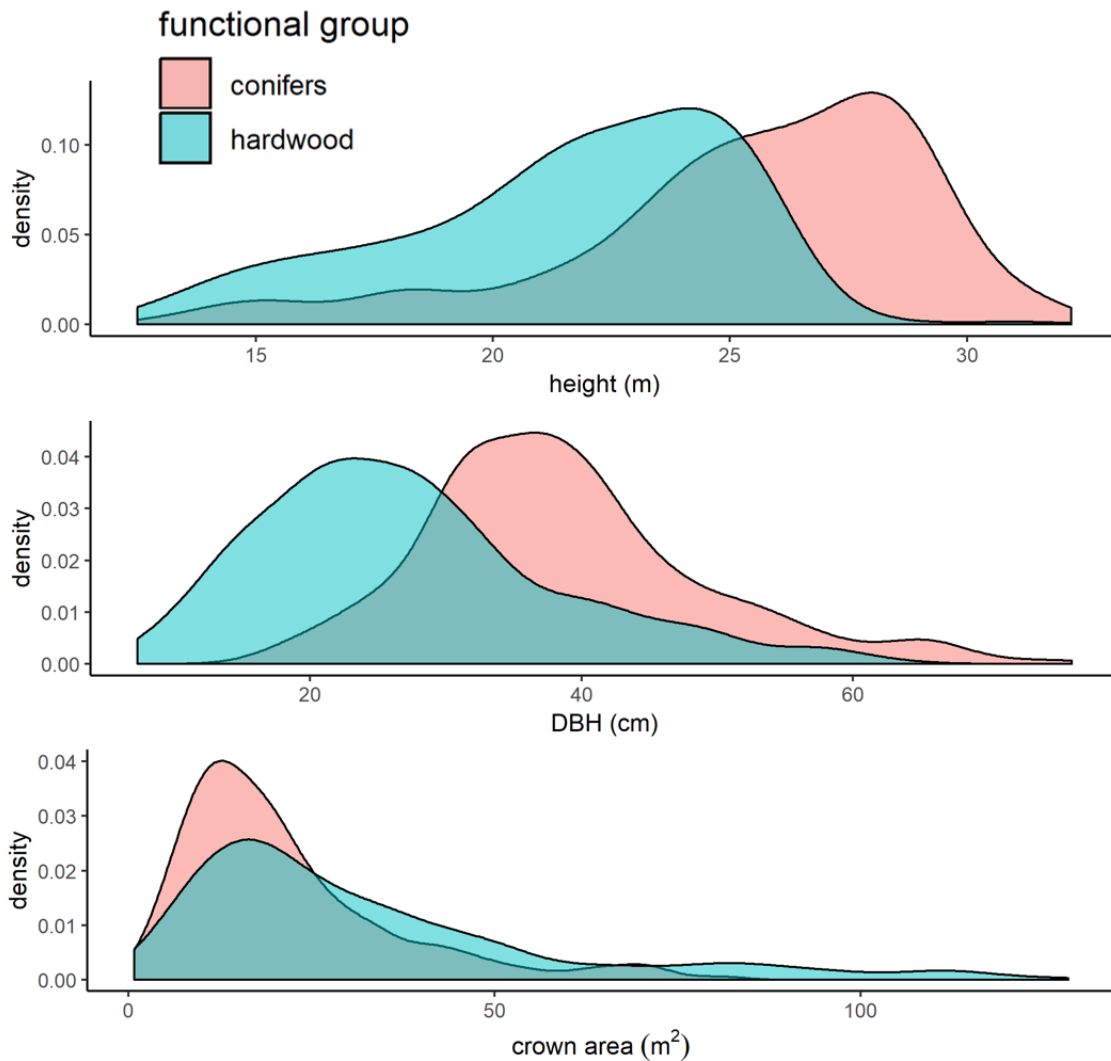


Figure 4: Density distribution of tree-level variables showing differences between conifer and hardwood functional groups. Conifers tend to have high diameter at breast height (DBH) and crown height values, while hardwoods tend to have larger crown area values.

Automated Crown Delineation Accuracy

Differences in methods and influence of parameter tuning

The influence of *generalized* parameter tuning compared to default parameters varied by method (**Table 2**). LI improved by 17% to achieve the highest *generalized* parameter accuracy (55%). SWS was particularly sensitive to parameterization, and overall accuracy improved from 8% to 49% compared to *default* parameters. In contrast, MCWS – which differs from SWS only in having a priority seed point – was relatively robust against parameterization tuning. MCWS achieved 49% overall accuracy with default parameters and only improved by 6% following tuning. SILVA and DALPONTE were similarly robust and *generalized* tuning of parameters only marginally improved accuracy (+ 1-2%). While further *plot-tuning* of method parameters only marginally improved overall accuracy scores (+2-6%), I chose to continue the analyses using *plot-tuned* results because plot-level accuracy (supplemental **Table 5**) improved by as much as 36% (LI) and because I was interested in understanding the factors that influenced the highest quality delineations.

Overall and plot-level accuracy

Following *plot-tuning* overall accuracy and plot-level accuracy did not vary substantially across delineation methods. Overall accuracy ranged from 51% by SWS to 59% by LI. Though LI was marginally more accurate (+4%) than the second highest overall accuracy (MCWS: 55%), it came at a substantial increase in processing time and complexity of input parameters (and necessarily require parameter tuning to achieve high accuracy).

Plot-level accuracy ranged from 27% (DALPONTE and SWS) to 90% (MCWS), and the difference between the most- and least- accurately delineated plot was >40% for all methods.

Plot-level accuracy was similarly wide-ranged for all methods (supplemental *Figure 10*), and significantly related to conifer fraction ($p < 0.05$) for all methods.

Table 2: Overall site accuracy (%) of five different automated crown delineation techniques. The table included *default*, *generalized*, and *plot-tuned* parameters. ‡ Conifer and hardwood accuracies are from *plot-tuned* model runs.

	Default	Generalized	Plot-tuned	Conifer [‡]	Hardwood [‡]
MCWS	0.49	0.53	0.55	0.65	0.40
SWS	0.08	0.49	0.51	0.54	0.46
DALPONTE	0.46	0.48	0.52	0.63	0.38
SILVA	0.48	0.49	0.54	0.67	0.39
LI	0.38	0.55	0.59	0.69	0.46

Differences in accuracy across species

All methods more accurately delineated conifer crowns (mean 64%) than hardwood crowns (mean 42%). Each method had trade-offs in accuracy at the species level, and no single method stood out as having the highest accuracy across all species (*Figure 5*). For example, SILVA delineated red pine especially well (81%), but had consistently low hardwood accuracy scores. While SWS, which had the lowest red pine accuracy (53%), excelled at delineating red oak in comparison to other methods (+9%).

Hemlock accuracy ranged from 76% (LI) to 56% (SWS). White pine accuracy ranged from 62% (MCWS) to 57% (SILVA). Spruce spp. accuracy ranged from 57% (MCWS) to 21% (LI and SWS), though only 13 spruce were present in the plots. Red maple accuracy ranged from 53% (LI) to 45% (DALPONTE). Red oak accuracy ranged from 48% (SWS) to 28% (MCWS).

Other hardwood species (birch spp., black oak, white ash, and black cherry) accuracy ranged from 40% (LI) to a low of 15% (DALPONTE)

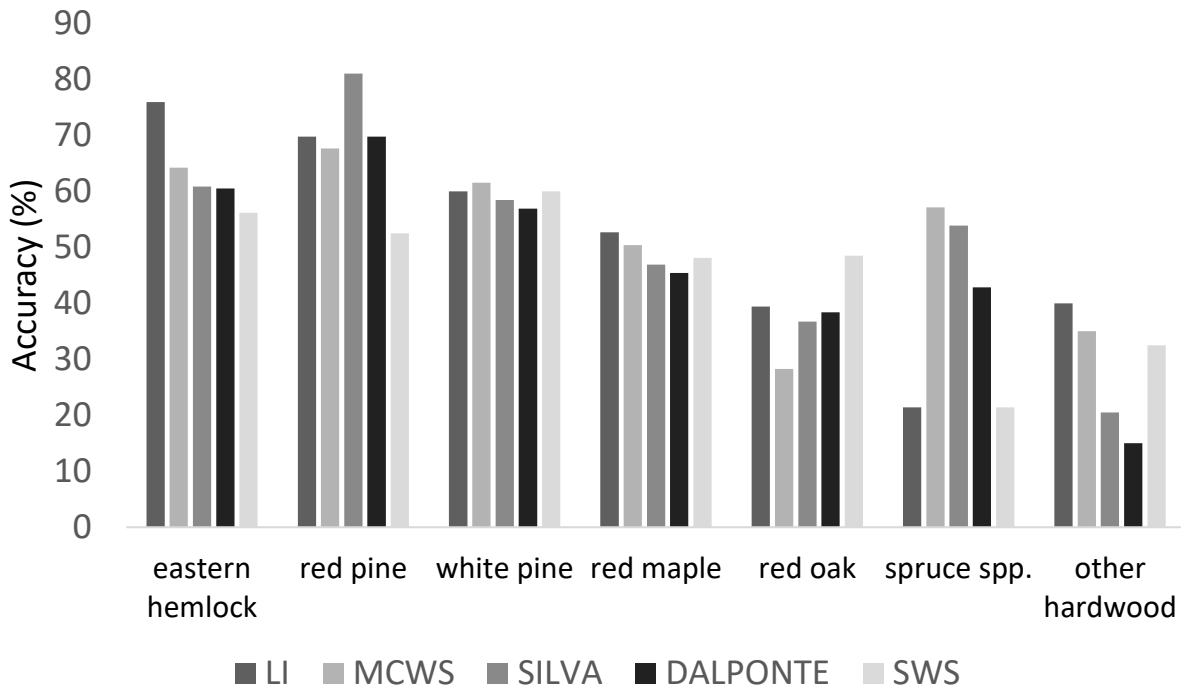


Figure 5: All automated crown delineation methods showed similar species level accuracy. Generally, conifer species (eastern hemlock, red pine, white pine and spruce) were more accurately delineated than hardwood species.

Variables Influencing Accurate Automated Crown Delineation

Linear regressions

Five plot-level variables (J, TPP, rumple, H, and AGI) were found to be significant ($p < 0.05$) in at least one univariate regression (**Figure 6** Error! Reference source not found.). All five variables were included in the multivariate global model. However, TPP and AGI were highly correlated ($r = 0.97$), and H and J were highly correlated ($r = 0.94$). To reduce VIF values to below 10, I removed TPP and H from the analysis. For each of the five multivariate regression analyses, the model including only J was selected as the best model, and this relationship

between accuracy and J was significant ($p < 0.05$) for all models (supplemental material: *Table 4*).

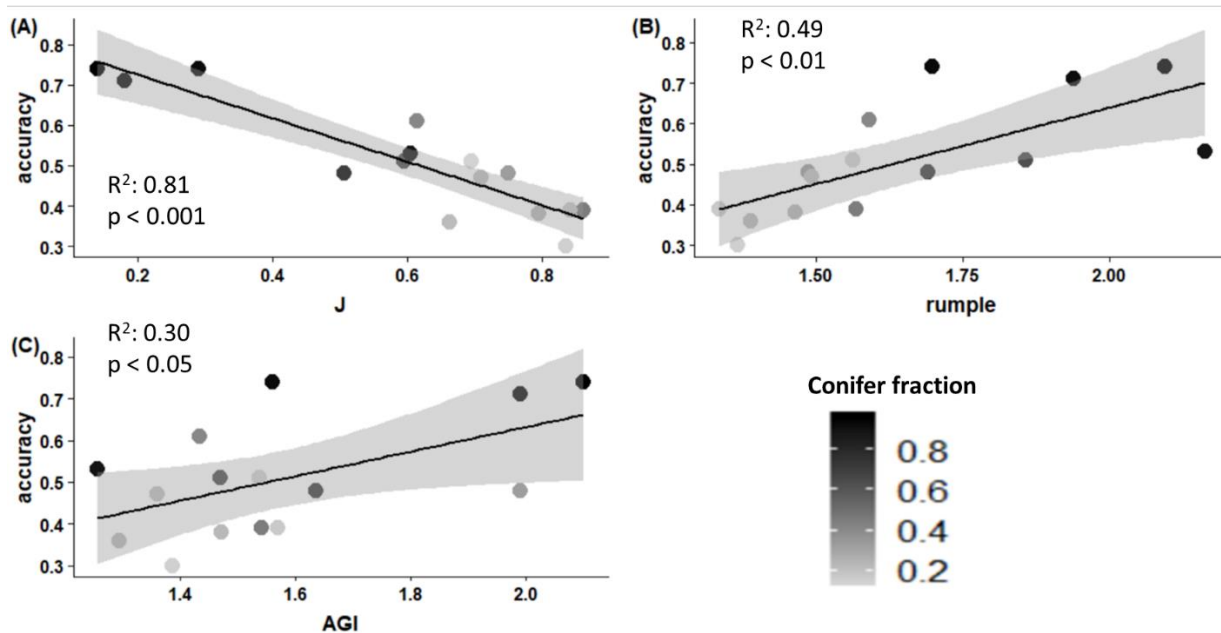


Figure 6: Linear regression analysis for plot-level variables and accuracy of one of the automated crown delineation methods (DALPONTE). Points are colored to show fraction of conifer crown area per plot (conifer fraction). The relationship between accuracy and evenness (J) was significant ($p < 0.05$) across all methods. However, the relationship between accuracy and aggregation index (AGI) was only significant for DALPONTE AND SILVA, and the relationship between accuracy and rumple index was only significant for DALPONTE, SIVLA and LI.

Logistic Regressions

Global logit models consisted of tree-level variables (DBH, height, and crown area) and the plot-level variables (rumple, J and AGI) identified in the linear regression analyses. Results of the final logit models are shown in *Table 3*. Cross validation model accuracy ranged from 61% (MCWS) to 70% (SWS), suggesting that while I captured the most impactful variables in predicting crown delineation, there may be additional factors unaccounted for in my analysis.

There was no single variable that was included in all five models. However, all but one model (SWS) consisted of at least one tree-level variable related to tree size and one plot-level variable related to tree arrangement.

Table 3: Results of the logit models assessing the important tree- and plot-level variables influencing the odds of successful individual tree crown delineation. All variables were standardized prior to analyses. The table includes the 10-fold cross-validation (CV %) model accuracy estimates, coefficients of variables in the models and the corresponding standard error (SE) (*p < 0.05, **p < 0.01, ***p < 0.001).

	CV %	Coefficient	SE (Coef)	Z value	p-value	
MCWS	60.77					
Intercept		0.19	0.16	1.16	0.25	
Crown Area		-0.38	0.11	-3.41	0.00	***
DBH		0.42	0.14	3.06	0.00	**
Height		0.39	0.28	1.39	0.16	
J		-0.68	0.26	-2.64	0.01	**
Rumple		-0.49	0.26	-1.89	0.06	.
DALPONTE	62.00					
Intercept		0.12	0.09	1.35	0.18	
AGI		0.36	0.12	2.88	0.00	**
DBH		0.60	0.11	5.51	0.00	***
J		-0.25	0.12	-2.11	0.03	*
SWS	70.00					
Intercept		-0.10	0.33	-0.30	0.76	
Crown Area		0.76	0.12	6.39	0.00	***
Height		1.25	0.25	4.91	0.00	***
SILVA	65.32					
Intercept		0.27	0.20	1.33	0.18	
AGI		0.47	0.21	2.21	0.03	*
Height		1.04	0.24	4.37	0.00	***
LI	61.54					
Intercept		0.41	0.11	3.78	0.00	***
Crown Area		-0.20	0.10	-1.97	0.05	*
DBH		0.50	0.11	4.39	0.00	***
J		-0.33	0.12	-2.75	0.01	**

All tree-level variables were important, each showing up in three of the five logit models, though not always together. Height and DBH always had a positive effect on the odds a crown would be successfully delineated. Crown area had a negative effect in two models, but it had a positive effect on the odds of delineation for the SWS method.

Plot-level variables were not consistently important across methods. Species evenness was the most important, showing up in three models, and each time having a negative effect on crown delineation accuracy ($p < 0.05$). AGI was included as positively affecting delineation in two models ($p < 0.05$), while rumple was only included in one model and negatively affected delineation odds ($p = 0.06$).

Discussion

Automated crown delineation remains difficult to apply in closed canopy mixed-species forests. Despite parameter tuning, none of the methods produced high accuracy across all plots, and there was relatively little difference between crown delineation methods. I found that all methods delineate conifer species better than hardwood species, and that accuracy of each method varied similarly across plots. Thus, it is evident that the ability to delineate crowns is not strongly driven by methodological differences, but instead driven by differences in conifer and hardwood functional groups. Conifers and hardwoods have developed traits that distinguish their ability to compete for resources and respond to disturbance and competition. In turn these traits influence tree height, crown architecture (crown spreading and leaf-display), and how crowns interact with neighboring crowns.

Tree Architecture

Tree size

I found that taller trees and larger diameter trees were more likely to be correctly delineated. This is in part because large trees often hold dominant positions in the canopy and tend to have more symmetrical crown shape (Muth and Bazzaz, 2003). Yet, this is also because conifers in the canopy tended to be taller and have larger diameters (**Figure 4**). Conifer species identified on the plots have lower average wood density (specific gravity) than the hardwood

species (Ducey and Knapp, 2010), which is energetically efficient for height growth (Anten and Schieving, 2010; Horn, 1971). In higher diameter size classes conifers diverge from hardwoods, growing taller (Ducey, 2012).

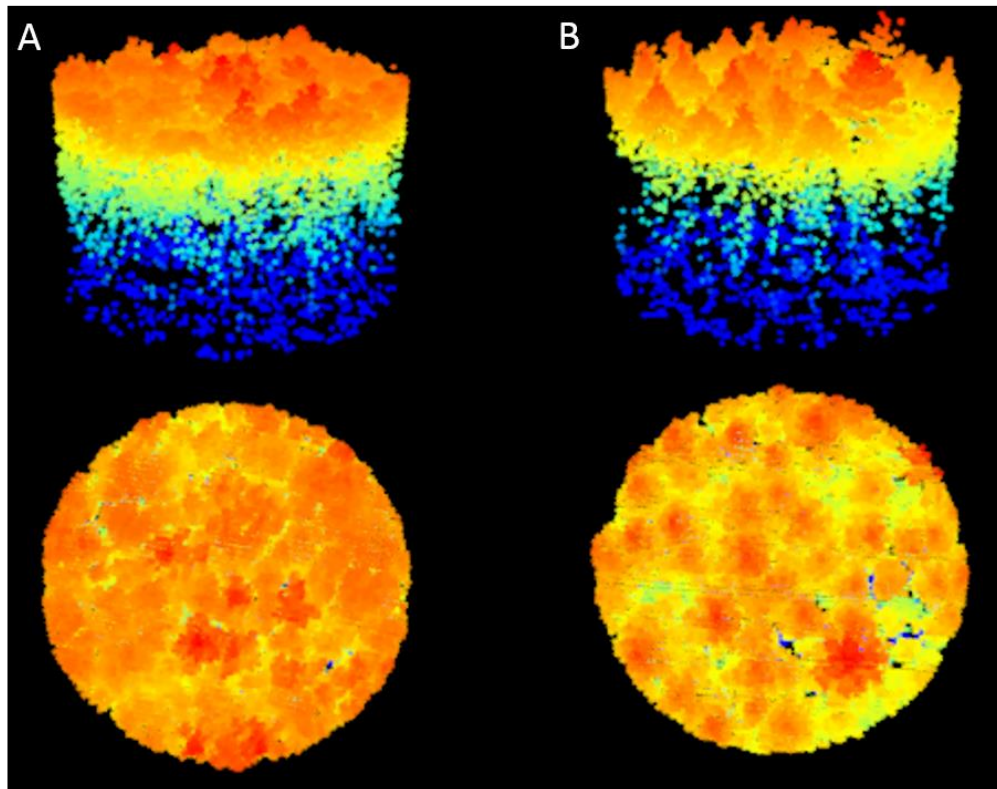


Figure 7: G-LiHT LiDAR point cloud comparison highlighting the differences in structure between a hardwood dominated stand (A) and a conifer dominated stand (B). Warmer colors represent higher points in the canopy. The conifer dominated stand exhibits higher canopy rumple, and uniformity of crown shape. The conical, less-plastic shape of conifer crowns may also reduce canopy space filling efficiency.

Conifers, especially white pine, are larger (diameter and height) because of site history and growth strategy. Much of the northeastern United States landscape has been shaped by historical land use (Foster et al., 1998; Thompson et al., 2013). White pine are successful colonization of disturbed sites, and many of the large white pine are old-field pines that invaded

agricultural and pastoral fields following abandonment in the mid-1800s (Abrams, 2001). Low density wood, and relatively high photosynthetic rates (Anten and Schieving, 2010; Brodribb et al., 2012) allow pine to achieve rapid vertical growth, and they continue to avoid direct competition by occupying a higher canopy stratum than hardwoods. On a canopy height model, emergent white pine appear as hotspots (supplemental **Figure 13**) because they often stand five or more meters above the continuous canopy; thus, they are easily detected and delineated by automated crown delineation methods.

Crown Spread

I found smaller crowns were more likely to be successfully delineated, and similar to height this is likely related to differences between conifers and hardwoods. Many mid- and shade tolerant hardwood species have weak apical control that results in plagiotropic growth forms (Pretzsch and Rais, 2016). Weak apical control allows multiple stems to compete for a dominant terminal position, the result of which can be a broad and flat crown, often with forked trunks and multiple differentiated sections within a single crown (i.e. crown splitting).

Conifer crowns tend to spread less than hardwood crowns, though it is possible to find white pine or hemlock that are comparable in spread to hardwood crowns. However, conifers maintain a more rigid, apically controlled growth form, and are less likely to exhibit crown plasticity (Strigul et al., 2008; Vincent and Harja, 2008). This results in a singularly defined orthotropic bole and the characteristically conical crown shape, and it far rarer to find conifers with forked trunks and split crowns.

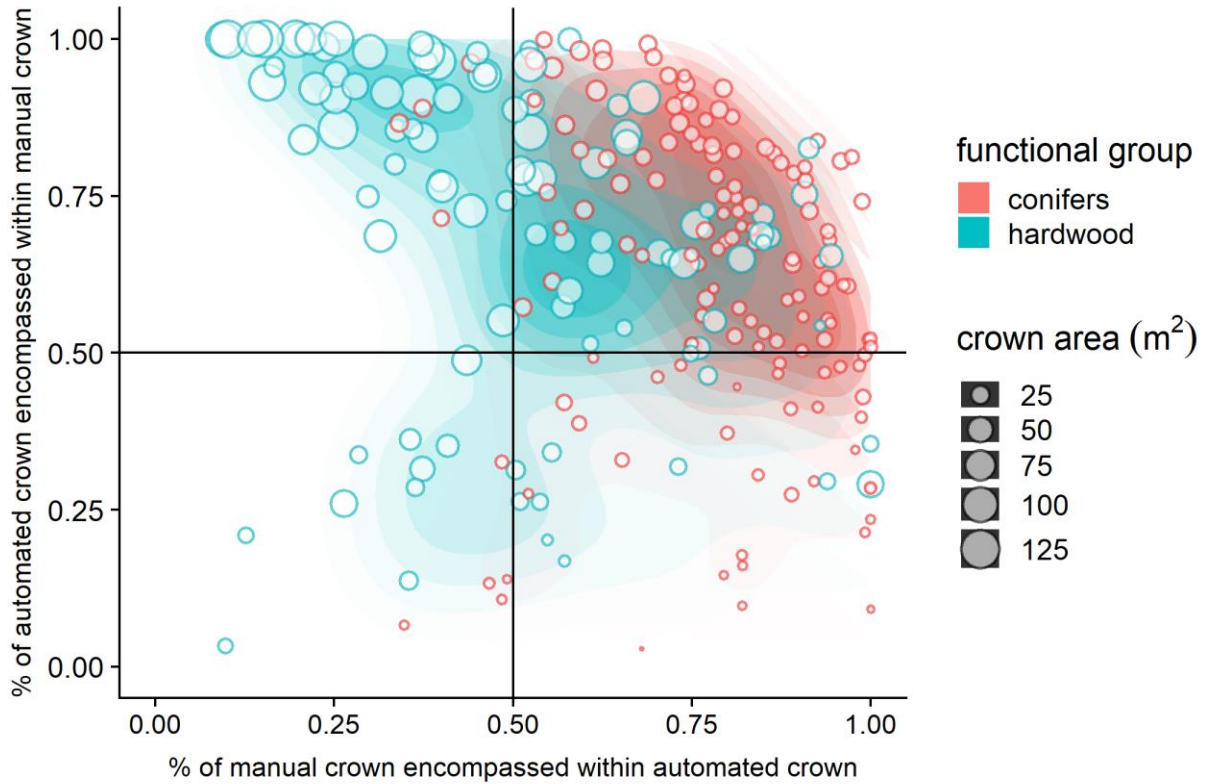


Figure 8: Two-dimensional density plot showing different patterns of crown delineation accuracy between conifer and hardwood functional groups. The circles provide crown size comparison for two end member species: red pine (shown in red circles) and red oak (shown in blue circles). This figure corresponds with delineation categories described in Figure 3: the top right quadrant signifies true delineations, the top left signifies over-segmentation, the bottom right signifies under-segmentation, and the bottom left signifies false positive. This figure shows data generated from the DALPONTE method, though all methods show similar patterns.

The ability to spread branches laterally is associated with wood density. Wood density is correlated with structural properties, including resistance to splitting, rupture stress, dynamic breakage, and increased elasticity (Chave et al., 2009). While low density wood is a lower carbon-cost approach to attain vertical expansion, hardwood species with denser wood can expand lateral branching without compromising structural integrity (Anten and Schieving, 2010; Horn, 1971). This is in agreement with crown radius – DBH allometric equations developed by

Sullivan *et al.* (2017) at the Harvard Forest. They found the crown radius slope to be steeper for hardwoods than conifers, and that this relationship was related to wood specific gravity.

Red oak, in particular, often have substantial crown spread and split crowns. This type of architecture presents two major challenges for automated tree crown delineation: 1) It is difficult to define a singular local maximum and 2) crowns either interdigitate with neighboring crowns – resulting in under-segmentation, or crowns split – resulting in over-segmentation. I found all methods most often over-segmented red oak (**Figure 8**). My results agree with other studies that found hardwood canopies are often over-segmented (Zhen *et al.*, 2016).

Mechanical interaction

Mechanical interactions between neighboring crowns is another major dynamic controlling lateral branch expansion, perhaps even more than resource competition (Hajek *et al.*, 2015). Crown shyness – gaps that form between adjacent crowns, often of the same species – can result from mechanical bud abrasion and branch damage during crown collisions (Putz *et al.*, 1984). While mechanical interactions occur between all adjacent crowns in closed-canopy stands, canopy gap persistence (i.e. crown shyness) is controlled by branch fragility and rates of regrowth following lateral branch damage (Hajek *et al.*, 2015).

Crown shyness is especially visible in red pine dominated plots (supplemental **Figure 14**), which were placed in an even-aged remnant pine plantation (Rainey *et al.*, 1999). Crown shyness is a common occurrence in even-aged conifer dominated stands (Goudie *et al.*, 2009), and shyness likely contributed to not only the high accuracy in these plots (as high as 80%), but also the fidelity of the delineations, because gaps between adjacent crowns creates defined borders for delineation (**Figure 8**). In comparison to hardwood species with strong, dense branches (e.g. red oak), red pine is more susceptible to collision damage. High height:diameter

ratios coupled with low wood density make the crowns of red pine susceptible to wind damage (Wonn and O'Hara, 2001) through increased crown mobility and resulting high-impact crown collisions (Rudnicki et al., 2001).

A traits perspective

Major differences in tree architecture between conifers and hardwoods stem from differences in underlying traits. While in direct competition, hardwoods often outcompete conifers in nutrient rich environments (Oliver and Larson, 1996), conifers have evolved different trait adaptations to disturbance and tolerance to stress (Brodribb et al., 2012) that allow them to persist (and sometimes outcompete hardwoods) in temperate forests. Within the 'fast-slow' plant economic spectrum proposed by Reich (2014) many of the traits exhibited by conifers would be considered *slow* in comparison to hardwood traits.

Conifers – many of which have evolved in resource poor conditions – often invest in long-lasting low-nitrogen (N) foliage (Gower et al., 1995). Convergent leaf- and canopy-structural properties (conical crown shape, clumped foliage) promote light scattering and more even/diffuse light conditions throughout the canopy, which in turn increasing radiation use efficiency of low foliar N species (Cohen and Pastor, 1996; Gower et al., 1995). Further, Ollinger (2011) pointed out that plants grown (or adapted to grow) in resource poor conditions allocate fewer resources to wood vs foliage, constraining crown spread.

In contrast, hardwoods have developed a *fast* strategy where they invest in costly high-N deciduous foliage which turns over annually. To pay for the high carbon-cost investment, hardwoods must maximize direct light interception. Mid- and shade- tolerant hardwoods (red oak, red maple) achieve this by spreading their crowns to maximize foliage display on a more even plane.

Within Reich's (2014) plant economic spectrum fast-trait species should have lower density wood optimized to transport water, and one might also expect fast-trait species to reach taller heights to optimized high-N leaf display. However, conifers and hardwoods have different wood anatomy (e.g. tracheids vs. xylem vessels for water transport), which makes direct comparison difficult (Brodrigg et al., 2012). Further, while less dense wood of conifers allows comparable (or greater) height growth, it does so at a lower carbon-cost, which allows more carbon investment elsewhere (e.g. belowground in nutrient poor environments; Gower et al., 1995).

There is also considerable variation in traits within each functional group (supplemental **Figure 15**). While in comparison to hardwoods white pine may be considered *slow*, within conifers, white pine is undoubtedly *fast*, with higher foliar nitrogen, shorter leaf life-span and low-density wood. At HF, white pine can diverge from the typical conical shape seen in other conifers, displaying spreading and flat-topped crowns. If it were not for other characteristics (e.g. occupying a higher canopy stratum) it may have been more difficult to delineate pine. Within hardwoods, early successional species (aspen, birch) have comparably high foliar N and low wood density. Where oaks and maples spread, these species invest in rapid vertical growth and very modest crown spread, and this combination of traits may result in easier ITCD, though this study did not permit me to investigate this. Thus, it appears that while the 'fast-slow' traits perspective provides an interesting lens to view crown architecture as it relates to crown delineation, there is considerable variation in traits, and perhaps even with inverse relationships within functional groups.

Species Evenness

I found that species evenness was the most important plot-level variable controlling crown delineation success. As species evenness decreased, the odds of successful delineation increased. Evenness was likely important because of 1) its negative relation to conifer fraction, and 2) a relationship between evenness and canopy space filling efficiency.

There was a strong relationship between species evenness and conifer fraction (supplemental **Figure 9**); the least even plots had the highest conifer fraction while the most even plots tended to have the lowest conifer fraction. It is important to note that two of the low evenness conifer plots were artificial in the sense that they are remnant red pine plantation, though red pine can grow naturally in monoculture. However, the other low evenness conifer plot was in a natural mature hemlock stand, a common occurrence in temperate forests (Small et al., 2005). It is not uncommon for conifer stands to have low evenness because of generally lower diversity (Augusto et al., 2014) of conifer species, and because needles of conifer species have high C:N ratio that can alter soil fertility conditions and deter hardwood establishment and growth (Brodribb et al., 2012).

Despite the evident influence of conifer fraction, the evenness – accuracy relationship may also be reflective of increased efficiency of canopy space filling (i.e. crown packing) in higher diversity plots. Recent work has shown that crown packing increases with species diversity (Jucker et al., 2015; Pretzsch, 2014), and that neighborhood species diversity also has a positive impact on individual tree productivity (Fichtner et al., 2018, 2017). In low diversity stands, trees from the same species compete similarly for growing space (*sensu* Oliver & Larson, 1996), while in higher diversity stands, niche partitioning and complementarity of crown architecture promote partitioning of resources (Morin et al., 2011; Sapijanskas et al., 2012), allowing more efficient and complete use of available canopy space (Pretzsch and Schütze, 2016;

Williams et al., 2017). As plot diversity increases crown packing increases, and it becomes increasingly difficult to differentiate neighboring crowns (*Figure 7*).

To further investigate the potential relationship between species evenness and crown packing, I calculated plot NDVI from the G-LiHT hyperspectral data as a proxy estimate of leaf area index and foliar density (Qiao et al., 2019), assuming increased crown packing would be related to increased LAI. I found evenness is strongly related to NDVI ($p < 0.001$; $R^2: 0.81$). However, because NDVI is also related to conifer fraction (Waring et al., 1995), I performed a partial correlation test. I found that after accounting for conifer fraction, NDVI was still positively correlated ($r: 0.58$) with species evenness, lending support to the idea that the evenness - accuracy relationship is both a result of conifer fraction and increased crown packing in higher diversity plots.

A silver lining: where do these methods work?

I found automated LiDAR ITCD methods show great promise for delineation of large trees. Despite lower accuracy for smaller size trees, these results are encouraging given the important role large trees play in terrestrial ecosystems (Freckleton and Watkinson, 2001), especially in terms of carbon accumulation (Stephenson et al., 2014). I was able to delineate 62-70% of all trees ≥ 40 cm DBH, which is promising for the prospect of tree-centric carbon mapping (Coomes et al., 2017; Dalponte and Coomes, 2016).

I also found these methods to perform especially well in conifer dominated stands. In particular, the current ability to delineate mature eastern hemlock has implications for current research and conservation interests in monitoring and mapping hemlock wooly adelgid (HWA) infestations (Orwig et al., 2012). Given the impact HWA has on the structure and composition of

infested forests (Small et al., 2005), the scientific community should not hesitate to deploy existing crown delineation methods to aid in measuring and mapping HWA impacts.

Much of the northeast United States is still aggrading second growth forest (Thompson et al., 2013). However, while our plots cover a range of structure and composition, they are undoubtedly still just a sample of the different forest types found across the northeast. LiDAR-crown delineation methods are likely to show varying degrees of accuracy based on additional factors influencing structure, such as stage of forest succession (van Ewijk et al., 2013). Relatively young stands in stem-exclusion stage (*sensu* Oliver & Larson, 1996), are likely to be especially difficult to delineate because of high-stem density and intense competition, while mature- and old-growth stands may show opposite patterns. Given that stand structural complexity often increase with stand age (Bradford and Kastendick, 2010), with increased number of large trees (Lorimer and Frelich, 1998) and canopy surface complexity (Ogunjemiyo et al., 2005), I would expect mature- and old-growth stands to be delineated with higher accuracy.

Moving forward

LiDAR-based crown delineation methods have garnered substantial interest in recent years because of the ability to directly measure structural characteristics of tree crowns (Lindberg and Holmgren, 2017). However, these methods still struggle to delineate hardwood canopies. What many (deciduous) hardwood crowns lack in architectural distinction – that many conifer crowns have that lend towards LiDAR-based delineation – they make up for in phenology and spectral distinction.

Indeed, much of the information I relied upon to manually delineate tree crowns – subtle differences in hue and texture – is lost in a LiDAR CHM model. Even more information may be

available hyperspectral or multi-temporal RGB imagery (supplemental *Figure 12*). Many studies have shown great success for spectrally distinguishing canopy species using hyperspectral (e.g. Shi et al., 2018) and multi-temporal imagery (Fang et al., 2018), while fewer studies have made use of this wealth of information available to delineate mixed- and hardwood- dominated forests (Maschler et al., 2018; Yang et al., 2017).

Undoubtedly, there has been work to use high resolution imagery for crown delineation, and it was the focus during the genesis of this research topic (Lamar et al., 2005; Leckie et al., 2004). However, many of studies often relied on panchromatic (Palace et al., 2008) or single band imagery (Ke and Quackenbush, 2011). Despite the limitations of spectral methods (Dalponte et al., 2015), integration of spectral characteristics into crown delineation methods would likely improve the ability to differentiate neighboring crowns that would otherwise be under-segmented or group crowns that would otherwise be over-segmented. Future work should focus on developing spectral- or integrated LiDAR-spectral delineation methods. The widespread availability of spectral platforms – including high-resolution spaceborne platforms – adds incentive to develop effective methods because of the potential to apply methods broadly.

Conclusion

The ability to automatically delineate individual tree crowns in all types of forests would be a major step forward for remote sensing-based ecology. I found that crown delineation remains difficult in closed-canopy mixed species forests of the northeastern United States. While LiDAR-based methods work well in conifer dominated plots, they are somewhat less effective in hardwood dominated plots, which may limit the applicability of these methods over broad spatial scales. Overall, discrepancies in accuracy appears to be driven by differences in underlying traits controlling tree architecture and how trees interact with each other in close proximity. LiDAR

methods work especially well in conifer dominated stands with distinct crown architecture. While hardwoods often lack the same structural distinction, they have unique phenology that may be exploited to improved delineation techniques. My work points towards a need to develop crown delineation techniques that integrate both structural and spectral characteristics to effectively delineate mixed species stands.

Supplemental Material

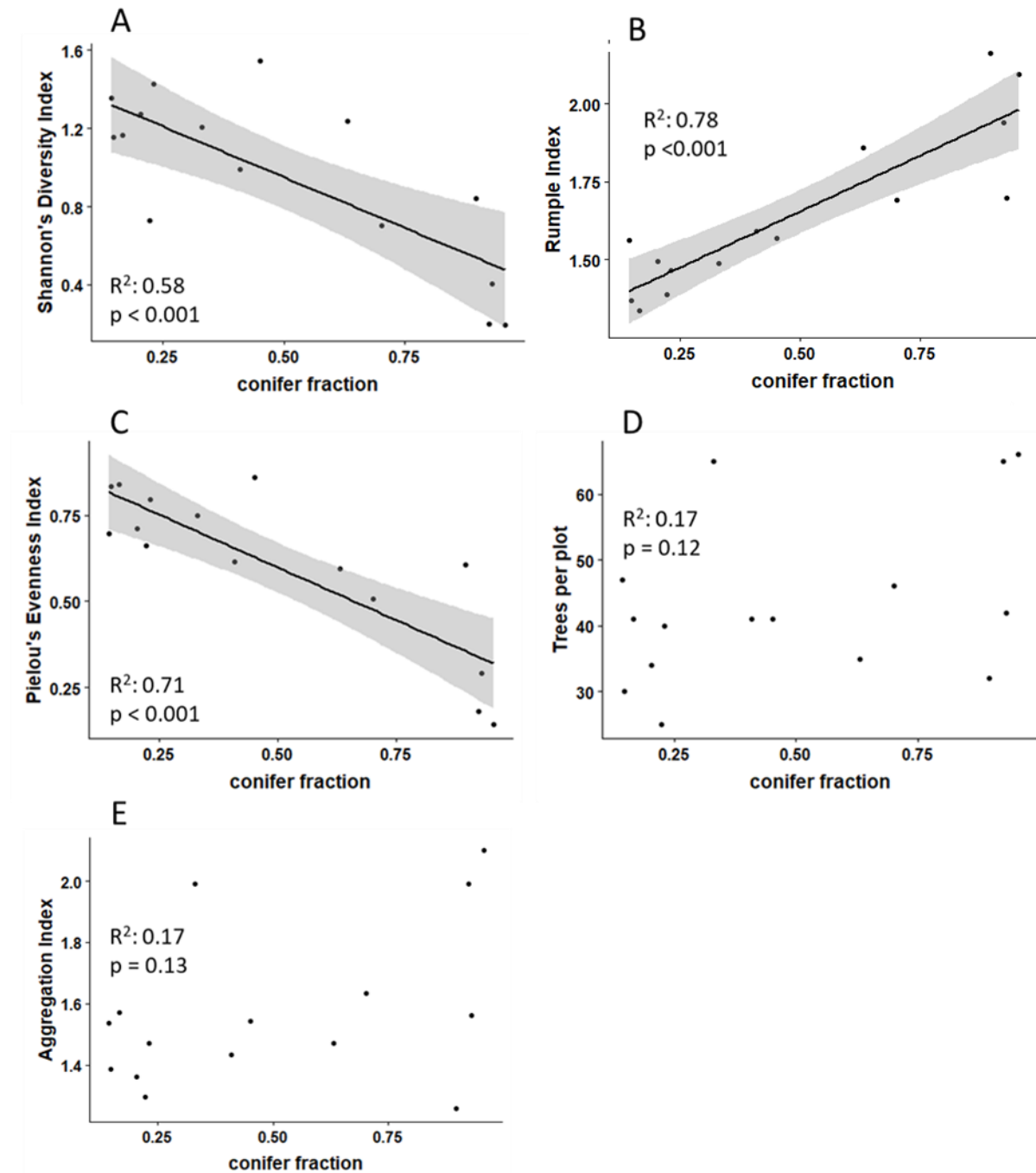


Figure 9: Relationships between the fraction of conifer crown area per plot (conifer fraction) and Shannon's Diversity Index (A), Rumple Index (B), Pielou's Evenness Index (C), trees per plot (D), and Aggregation Index (E).

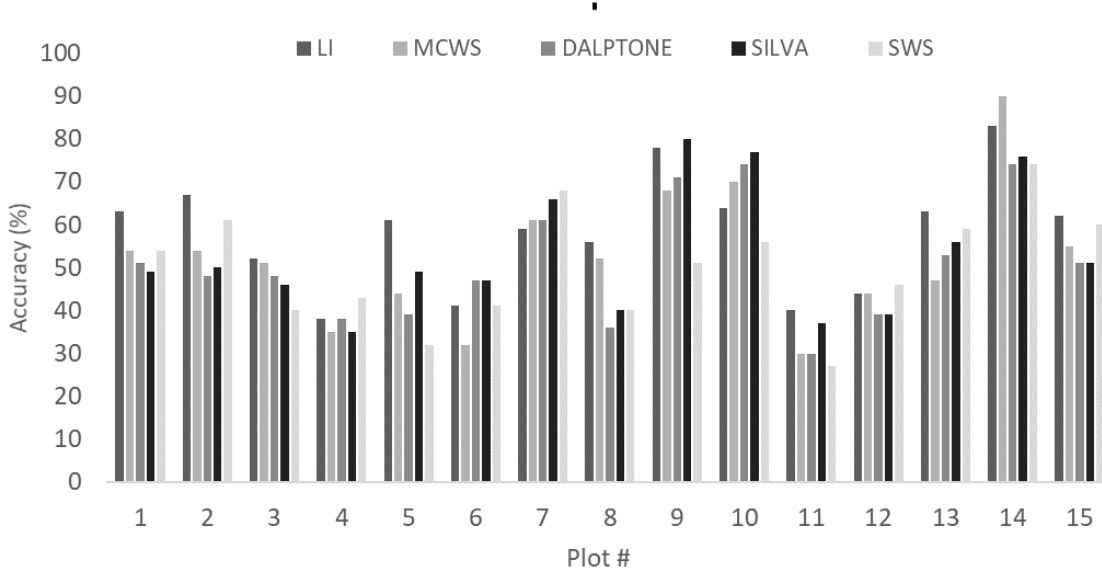


Figure 10: Following parameter tuning, plot-level accuracy varied similarly by methods across plot, indicating that accuracy is largely controlled by the structure and composition of the plots rather than methodological differences.

Table 4: Results from multivariate models assessing the influence of plot-level metrics on overall accuracy of five automated crown delineation methods. The table includes the coefficients of variables in the models and the corresponding standard error (SE) (*p < 0.05, **p < 0.01, ***p < 0.001).

	Coefficient	SE (Coef)	t value	p-value	
MCWS					
Intercept	0.52	0.02	21.30	0.0000	***
J	-0.13	0.03	-4.99	0.0002	***
SWS					
Intercept	0.50	0.03	17.69	0.0000	***
J	-0.08	0.03	-2.71	0.0177	*
DALPONTE					
Intercept	0.51	0.02	31.33	0.0000	***
J	-0.13	0.02	-7.50	0.0000	***
SILVA					
Intercept	0.53	0.02	30.16	0.0000	***
J	-0.13	0.02	-7.29	0.0000	***
LI					
Intercept	0.53	0.02	30.16	0.0000	***
J	-0.13	0.02	-7.29	0.0000	***



Figure 11: September UAV image collected over the MegaPlot showing the location of the fifteen plots used in this study.

Table 5: Results from accuracy assessment from five different automated crown delineation method at the plot level. The table includes plot-tuned, generalized, and default parameter accuracy.

	Plot	1	2	3	4	5	6	7	8	9	10	11	12	13	14	15
<i>LI</i>	Plot-tuned	0.63	0.67	0.52	0.38	0.61	0.41	0.59	0.56	0.78	0.64	0.40	0.44	0.63	0.83	0.62
	Generalized	0.63	0.67	0.51	0.30	0.59	0.41	0.59	0.20	0.75	0.64	0.27	0.41	0.53	0.83	0.51
	Default	0.34	0.35	0.34	0.25	0.32	0.29	0.49	0.28	0.54	0.39	0.20	0.32	0.34	0.50	0.47
	Plot-tuned	0.49	0.50	0.46	0.35	0.49	0.47	0.66	0.40	0.80	0.77	0.37	0.39	0.56	0.76	0.51
	Generalized	0.43	0.43	0.46	0.28	0.39	0.29	0.61	0.20	0.72	0.70	0.27	0.37	0.44	0.76	0.51
	Default	0.43	0.39	0.45	0.23	0.37	0.29	0.54	0.16	0.72	0.68	0.27	0.37	0.44	0.71	0.47
<i>DALPONTE</i>	Plot-tuned	0.51	0.48	0.48	0.38	0.39	0.47	0.61	0.36	0.71	0.74	0.30	0.39	0.53	0.74	0.51
	Generalized	0.49	0.48	0.48	0.28	0.39	0.32	0.61	0.24	0.66	0.68	0.27	0.34	0.34	0.71	0.51
	Default	0.43	0.46	0.46	0.20	0.39	0.32	0.56	0.24	0.66	0.65	0.27	0.34	0.34	0.67	0.47
	Plot-tuned	0.54	0.61	0.40	0.43	0.32	0.41	0.68	0.40	0.51	0.56	0.27	0.46	0.59	0.74	0.60
	Generalized	0.49	0.59	0.40	0.40	0.32	0.41	0.66	0.40	0.49	0.52	0.23	0.46	0.59	0.74	0.60
	Default	0.20	0.15	0.02	0.03	0.05	0.00	0.07	0.08	0.02	0.02	0.00	0.00	0.22	0.38	0.04
<i>MCW5</i>	Plot-tuned	0.54	0.54	0.51	0.35	0.44	0.32	0.61	0.52	0.68	0.70	0.30	0.44	0.47	0.90	0.55
	Generalized	0.54	0.54	0.51	0.35	0.44	0.32	0.61	0.24	0.68	0.70	0.30	0.44	0.34	0.90	0.55
	Default	0.51	0.52	0.51	0.28	0.44	0.32	0.56	0.24	0.68	0.65	0.30	0.44	0.34	0.86	0.51

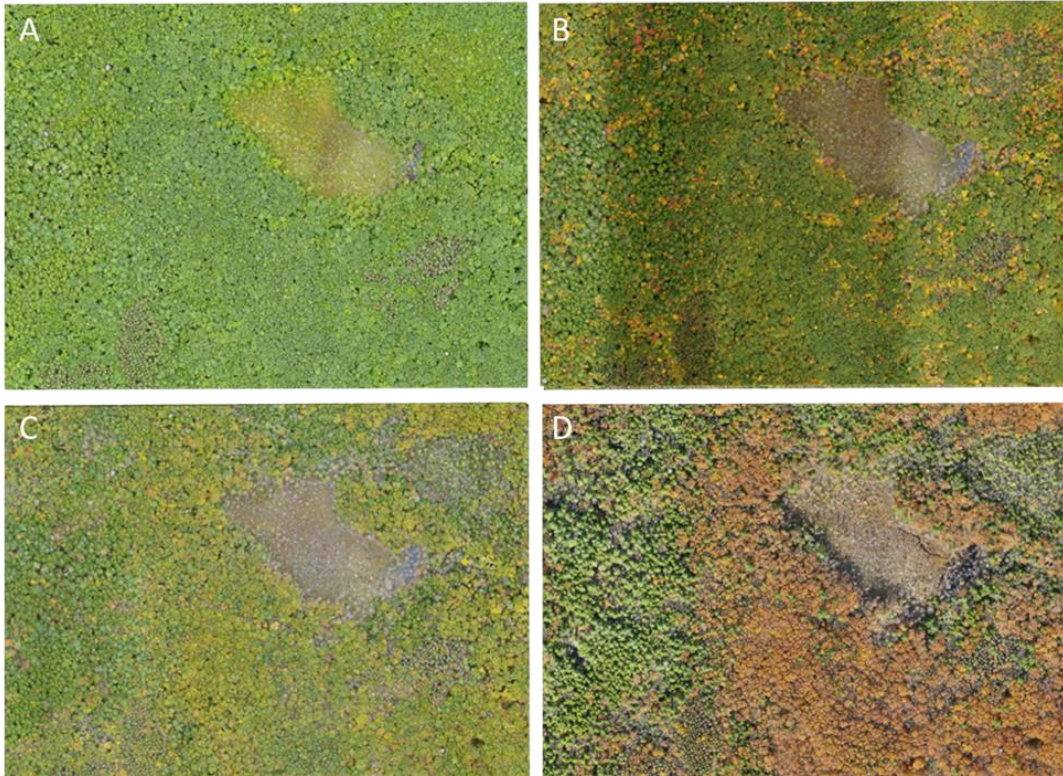


Figure 12: UAV imagery collected over the ForestGEO MegaPlot on September 13th (A), October 12th (B), October 22th (C) and November 4th (D). All these dates of imagery were used to during manual crown delineation interpretation. The images highlight differences in phenology that may be useful for future crown delineation work.

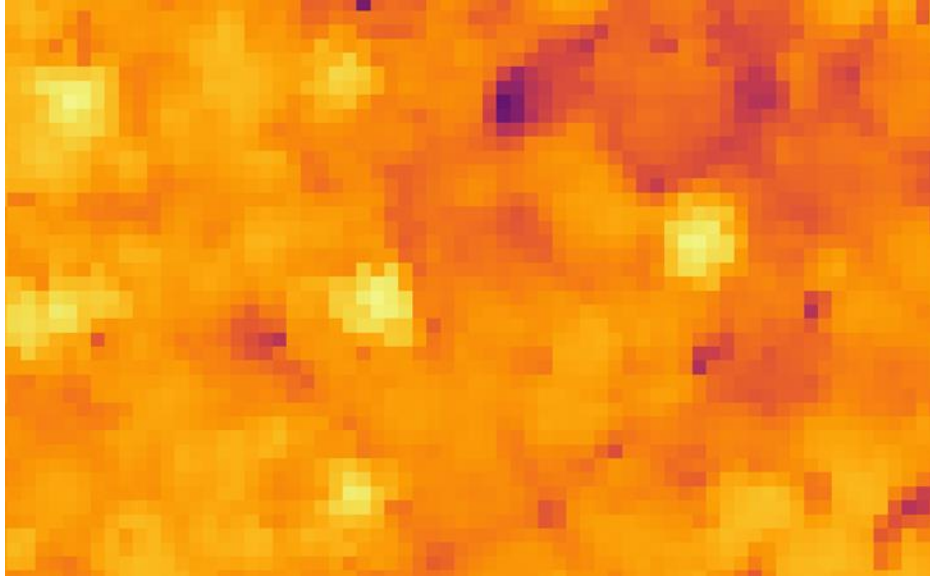


Figure 13: Emergent white pine crowns stand out as hotspots on a canopy height model. Low density wood allows white pine to grow taller than all other species in the Harvard Forest. They can often stand five or more meters above the continuous canopy.

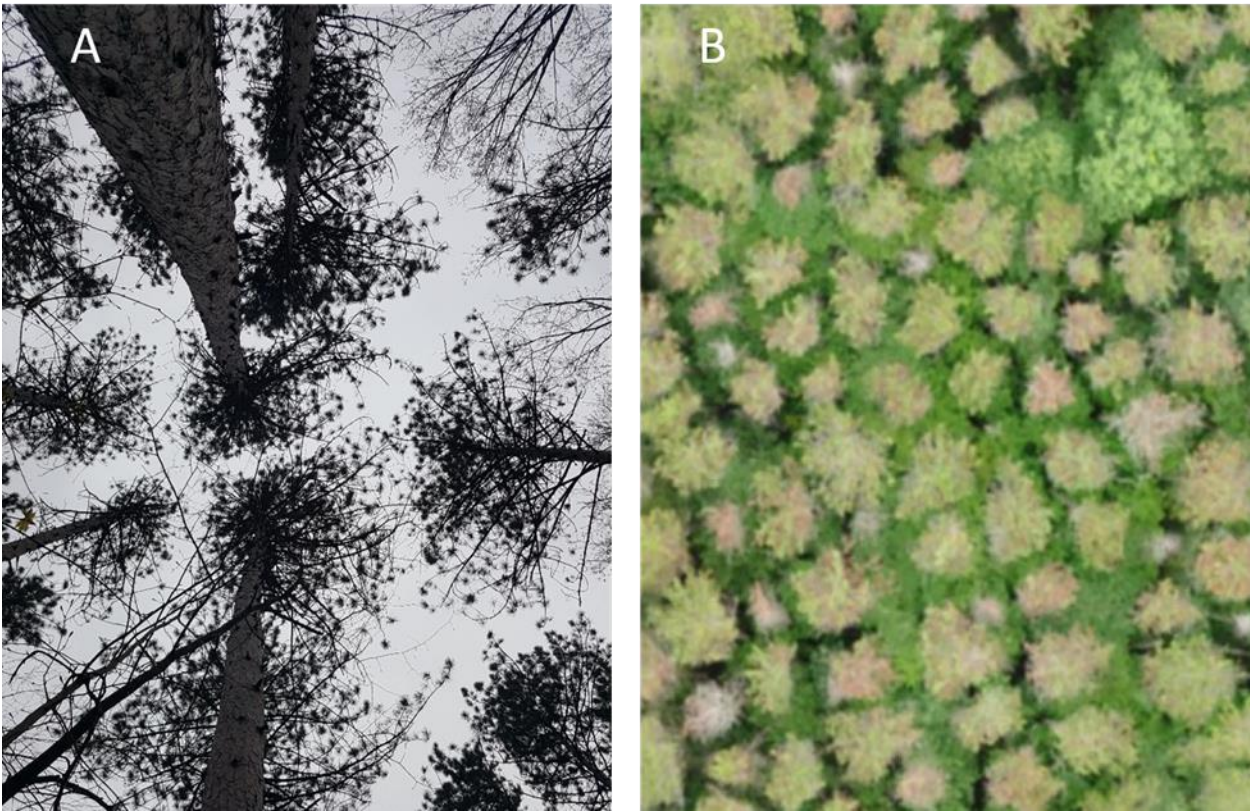


Figure 14: Red pine often exhibit crown shyness when grown in monoculture. Panel A shows crown shyness from below the canopy, while Panel B shows it from above the canopy.

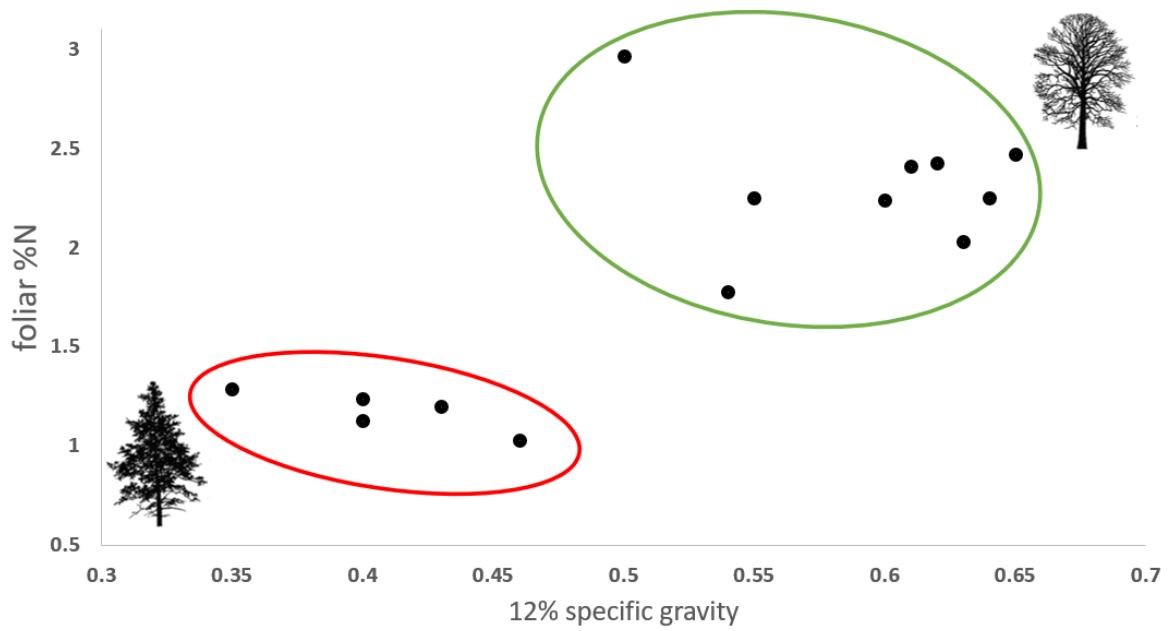


Figure 15: Conifer and hardwood functional groups show distinct differences in foliar nitrogen and wood density (specific gravity) that influence overall tree architecture and how they interact with neighboring crowns. There is also considerable variation of traits within functional groups. Average foliar %N values taken from Northeastern Ecosystem Research Cooperative (2010). Average specific gravity values taken from Ducey and Knapp (2010).

List of References

- Abrams, M.D., 2001. Eastern White Pine Versatility in the Presettlement Forest. *Bioscience* 51, 967–979. [https://doi.org/10.1641/0006-3568\(2001\)051\[0967:ewpvit\]2.0.co;2](https://doi.org/10.1641/0006-3568(2001)051[0967:ewpvit]2.0.co;2)
- Anderson-teixeira, K.J., Davies, S.J., Bennett, A.M.Y.C., Muller-landau, H.C., Wright, S.J., 2015. CTFS-ForestGEO : a worldwide network monitoring forests in an era of global change 528–549. <https://doi.org/10.1111/gcb.12712>
- Anten, N.P.R., Schieving, F., 2010. The Role of Wood Mass Density and Mechanical Constraints in the Economy of Tree Architecture. *Am. Nat.* 175, 250–260. <https://doi.org/10.1086/649581>
- Asner, G.P., Palace, M., Keller, M., Pereira, R., Silva, J.N.M., Zweede, J.C., 2002. Estimating Canopy Structure in an Amazon Forest from Laser Range Finder and IKONOS Satellite Observations I. *Biotropica* 34, 483. [https://doi.org/10.1646/0006-3606\(2002\)034\[0483:ecsiaa\]2.0.co;2](https://doi.org/10.1646/0006-3606(2002)034[0483:ecsiaa]2.0.co;2)
- Augusto, L., Davies, T.J., Delzon, S., de Schrijver, A., 2014. The enigma of the rise of angiosperms: Can we untie the knot? *Ecol. Lett.* 17, 1326–1338. <https://doi.org/10.1111/ele.12323>
- Ayrey, E., Fraver, S., Kershaw, J.A., Kenefic, L.S., Hayes, D., Weiskittel, A.R., Roth, B.E., 2017. Layer Stacking: A Novel Algorithm for Individual Forest Tree Segmentation from LiDAR Point Clouds. *Can. J. Remote Sens.* 43, 16–27. <https://doi.org/10.1080/07038992.2017.1252907>
- Bates, D., Maechler, M., Bolker, B., Walker, S., 2015. Fitting Linear Mixed-Effects Models Using lme4. *J. Stat. Softw.* 67, 1–48. <https://doi.org/doi:10.18637/jss.v067.i01>
- Bradford, J.B., Kastendick, D.N., 2010. Age-related patterns of forest complexity and carbon storage in pine and aspen–birch ecosystems of northern Minnesota, USA. *Can. J. For. Res.* 40, 401–409. <https://doi.org/10.1139/x10-002>
- Broadbent, E.N., Asner, G.P., Peña-Claros, M., Palace, M., Soriano, M., 2008. Spatial partitioning of biomass and diversity in a lowland Bolivian forest: Linking field and remote sensing measurements. *For. Ecol. Manage.* 255, 2602–2616. <https://doi.org/10.1016/j.foreco.2008.01.044>
- Brodribb, T.J., Pittermann, J., Coomes, D.A., 2012. Elegance versus Speed: Examining the Competition between Conifer and Angiosperm Trees. *Int. J. Plant Sci.* 173, 673–694. <https://doi.org/10.1086/666005>
- Burnham, K.P., Anderson, D.R., 2002. Model Selection and Multimodel Inference: A practical Information-theoretic Approach (2nd ed). Library of Congress Cataloging-in-Publication Data, Ecological Modelling. <https://doi.org/10.1016/j.ecolmodel.2003.11.004>
- Chave, J., Coomes, D., Jansen, S., Lewis, S.L., Swenson, N.G., Zanne, A.E., 2009. Towards a worldwide wood economics spectrum. *Ecol. Lett.* 12, 351–366. <https://doi.org/10.1111/j.1461-0248.2009.01285.x>

- Clark, M.L., Roberts, D.A., Clark, D.B., 2005. Hyperspectral discrimination of tropical rain forest tree species at leaf to crown scales. *Remote Sens. Environ.* 96, 375–398. <https://doi.org/10.1016/j.rse.2005.03.009>
- Clark, P.J., Evans, F.C., 1954. Distance to Nearest Neighbor As a Measure of Spatial Relationships in Populations. *Ecology* 35, 445–453.
- Cohen, Y., Pastor, J., 1996. Interactions Among Nitrogen , Carbon , Plant Shape , and Photosynthesis. *Am. Nat.* 147, 847–865.
- Cook, B.D., Corp, L.A., Nelson, R.F., Middleton, E.M., Morton, D.C., Mccorkel, J.T., Masek, J.G., Ranson, K.J., Ly, V., Montesano, P.M., 2013. NASA Goddard’s LiDAR, Hyperspectral and Thermal (G-LiHT) Airborne Imager. *Remote Sens.* 5, 4045–4066. <https://doi.org/10.3390/rs5084045>
- Coomes, D.A., Dalponte, M., Jucker, T., Asner, G.P., Banin, L.F., Burslem, D.F.R.P., Lewis, S.L., Nilus, R., Phillips, O.L., Phua, M.-H., Qie, L., 2017. Area-based vs tree-centric approaches to mapping forest carbon in Southeast Asian forests from airborne laser scanning data. <https://doi.org/10.1016/j.rse.2017.03.017>
- Crowley, K.F., Lovett, G.M., Arthur, M.A., Weathers, K.C., 2016. Long-term effects of pest-induced tree species change on carbon and nitrogen cycling in northeastern U.S. forests: A modeling analysis. *For. Ecol. Manage.* 372, 269–290. <https://doi.org/10.1016/j.foreco.2016.03.045>
- Dalponte, M., Coomes, D.A., 2016. Tree-centric mapping of forest carbon density from airborne laser scanning and hyperspectral data. *Methods Ecol. Evol.* 7, 1236–1245. <https://doi.org/10.1111/2041-210X.12575>
- Dalponte, M., Reyes, F., Kandare, K., Gianelle, D., 2015. Delineation of individual tree crowns from ALS and hyperspectral data: A comparison among four methods. *Eur. J. Remote Sens.* 48, 365–382. <https://doi.org/10.5721/EuJRS20154821>
- Ducey, M.J., 2012. Evergreenness and wood density predict height-diameter scaling in trees of the northeastern United States. *For. Ecol. Manage.* 279, 21–26. <https://doi.org/10.1016/j.foreco.2012.04.034>
- Ducey, M.J., Knapp, R.A., 2010. A stand density index for complex mixed species forests in the northeastern United States. *For. Ecol. Manage.* 260, 1613–1622. <https://doi.org/10.1016/j.foreco.2010.08.014>
- Fang, F., McNeil, B.E., Warner, T.A., Maxwell, A.E., 2018. Combining high spatial resolution multi-temporal satellite data with leaf-on LiDAR to enhance tree species discrimination at the crown level. *Int. J. Remote Sens.* 39, 9054–9072. <https://doi.org/10.1080/01431161.2018.1504343>
- Fichtner, A., Härdtle, W., Bruelheide, H., Kunz, M., Li, Y., Von Oheimb, G., 2018. Neighbourhood interactions driveoveryielding in mixed-species tree communities. *Nat. Commun.* 9. <https://doi.org/10.1038/s41467-018-03529-w>
- Fichtner, A., Härdtle, W., Li, Y., Bruelheide, H., Kunz, M., von Oheimb, G., 2017. From competition to facilitation: how tree species respond to neighbourhood diversity. *Ecol. Lett.*

- 20, 892–900. <https://doi.org/10.1111/ele.12786>
- Forrester, D.I., Benneter, A., Bouriaud, O., Bauhus, J., 2017. Diversity and competition influence tree allometric relationships – developing functions for mixed-species forests. *J. Ecol.* 105, 761–774. <https://doi.org/10.1111/1365-2745.12704>
- Foster, D.R., Motzkin, G., Slater, B., 1998. Land-Use History as Long-Term Broad-Scale Disturbance: Regional Forest Dynamics in Central New England. *Ecosystems*. <https://doi.org/10.1007/s100219900008>
- Freckleton, R.P., Watkinson, A.R., 2001. Asymmetric competition between plant species. *Funct. Ecol.* 15, 615–623. <https://doi.org/10.1046/j.0269-8463.2001.00558.x>
- Givnish, T.J., 2002. Ecological Constraints on the Evolution of Breeding Systems in Seed Plants: Dioecy and Dispersal in Gymnosperms. *Evolution* (N. Y). 34, 959. <https://doi.org/10.2307/2408001>
- Goudie, J.W., Polsson, K.R., Ott, P.K., 2009. An empirical model of crown shyness for lodgepole pine (*Pinus contorta* var. *latifolia* [Engl.] Critch.) in British Columbia. *For. Ecol. Manage.* 257, 321–331. <https://doi.org/10.1016/j.foreco.2008.09.005>
- Gower, S.T., Isebrands, J.G., Sheriff, D.W., 1995. Carbon Allocation and Accumulation in Conifers, in: *Resource Physiology of Conifers*. pp. 217–254.
- Hair, J.F., Anderson, R.E., Tatham, R.L., Black, W.C., 1995. *Multivariate Data Analysis*, 3rd ed. New York: MacMillian.
- Hajek, P., Seidel, D., Leuschner, C., 2015. Mechanical abrasion, and not competition for light, is the dominant canopy interaction in a temperate mixed forest. *For. Ecol. Manage.* 348, 108–116. <https://doi.org/10.1016/j.foreco.2015.03.019>
- Heip, C.H.R., Herman, P.M.J., Soetaert, K., 1998. Indices of diversity and evenness. *Océanis* 24, 61–87.
- Horn, H.S., 1971. *The adaptive geometry of trees*. Princeton University Press, Princeton, New Jersey.
- Houghton, R.A., 1995. Land-use change and the carbon cycle. *Glob. Chang. Biol.* 1, 275–287. <https://doi.org/10.1111/j.1365-2486.1995.tb00026.x>
- Jing, L., Hu, B., Noland, T., Li, J., 2012. An individual tree crown delineation method based on multi-scale segmentation of imagery. *ISPRS J. Photogramm. Remote Sens.* 70, 88–98. <https://doi.org/10.1016/j.isprsjprs.2012.04.003>
- Jucker, T., Bouriaud, O., Coomes, D.A., 2015. Crown plasticity enables trees to optimize canopy packing in mixed-species forests. *Funct. Ecol.* 29, 1078–1086. <https://doi.org/10.1111/1365-2435.12428>
- Kane, V.R., Gillespie, A.R., McGaughey, R., Lutz, J.A., Ceder, K., Franklin, J.F., 2008. Interpretation and topographic compensation of conifer canopy self-shadowing. *Remote Sens. Environ.* 112, 3820–3832. <https://doi.org/10.1016/j.rse.2008.06.001>
- Ke, Y., Quackenbush, L.J., 2011. A comparison of three methods for automatic tree crown

- detection and delineation from high spatial resolution imagery. *Int. J. Remote Sens.* 32, 3625–3647. <https://doi.org/10.1080/01431161003762355>
- Lamar, W.R., McGraw, J.B., Warner, T.A., 2005. Multitemporal censusing of a population of eastern hemlock (*Tsuga canadensis* L.) from remotely sensed imagery using an automated segmentation and reconciliation procedure. *Remote Sens. Environ.* 94, 133–143. <https://doi.org/10.1016/j.rse.2004.09.003>
- Leckie, D.G., Jay, C., Gougeon, F.A., Sturrock, R.N., Paradine, D., 2004. Detection and assessment of trees with *Phellinus weirii* (laminated root rot) using high resolution multi-spectral imagery. *Int. J. Remote Sens.* 25, 793–818. <https://doi.org/10.1080/0143116031000139926>
- Li, W., Guo, Q., Jakubowski, M.K., Kelly, M., 2012. A New Method for Segmenting Individual Trees from the Lidar Point Cloud. *Photogramm. Eng. Remote Sens.* 78, 75–84. <https://doi.org/10.14358/pers.78.1.75>
- Lindberg, E., Holmgren, J., 2017. Individual Tree Crown Methods for 3D Data from Remote Sensing. *Curr. For. Reports* 3, 19–31. <https://doi.org/10.1007/s40725-017-0051-6>
- Lorimer, C., Frelich, L.E., 1998. A structural Alternative to Chronosequence Analysis for Uneven-Aged Northern Hardwood Forests. *J. Sustain. For.* 6, 347–365. <https://doi.org/10.1300/J091v06n03>
- Lu, X., Guo, Q., Li, W., Flanagan, J., 2014. A bottom-up approach to segment individual deciduous trees using leaf-off lidar point cloud data. *ISPRS J. Photogramm. Remote Sens.* 94, 1–12. <https://doi.org/10.1016/j.isprsjprs.2014.03.014>
- Maschler, J., Atzberger, C., Immitzer, M., 2018. Individual tree crown segmentation and classification of 13 tree species using Airborne hyperspectral data. *Remote Sens.* 10. <https://doi.org/10.3390/rs10081218>
- McCune, B., Grace, J.B., 2002. *Analysis of Ecological Communities*. MjM Software Design, Glenden Beach, OR, US. [https://doi.org/10.1016/S0022-0981\(03\)00091-1](https://doi.org/10.1016/S0022-0981(03)00091-1)
- Morin, X., Fahse, L., Scherer-Lorenzen, M., Bugmann, H., 2011. Tree species richness promotes productivity in temperate forests through strong complementarity between species. *Ecol. Lett.* 14, 1211–1219. <https://doi.org/10.1111/j.1461-0248.2011.01691.x>
- Muth, C.C., Bazzaz, F.A., 2003. Tree canopy displacement and neighborhood interactions. *Can. J. For. Res.* 33, 1323–1330. <https://doi.org/10.1139/x03-045>
- NERC, 2010. *Compilation of foliar chemistry data for the northeastern United States and southeastern Canada*.
- Oberle, B., Ogle, K., Zanne, A.E., Woodall, C.W., 2018. When a tree falls: Controls on wood decay predict standing dead tree fall and new risks in changing forests. *PLoS One* 13, 1–22. <https://doi.org/10.1371/journal.pone.0196712>
- Ogunjemiyo, S., Parker, G., Roberts, D., 2005. Reflections in bumpy terrain: Implications of canopy surface variations for the radiation balance of vegetation. *IEEE Geosci. Remote Sens. Lett.* 2, 90–93. <https://doi.org/10.1109/LGRS.2004.841418>

- Oliver, C.D., Larson, B.C., 1996. *Forest Stand Dynamics*. John Wiley and Sons Inc., New York, NY.
- Oliver, C.D., Stephens, E.P., 1977. Reconstruction of a Mixed-Species Forest in Central New England. *Ecology* 58, 562–572. <https://doi.org/10.2307/1939005>
- Ollinger, S. V., 2011. Sources of variability in canopy reflectance and the convergent properties of plants. *New Phytol.* <https://doi.org/10.1111/j.1469-8137.2010.03536.x>
- Orwig, D., Ellison, A., 2015. Harvard Forest CTFS-ForestGEO Mapped Forest Plot since 2014.
- Orwig, D.A., Thompson, J.R., Povak, N.A., Manner, M., Niebyl, D., Foster, D.R., 2012. A foundation tree at the precipice: *Tsuga canadensis* health after the arrival of *Adelges tsugae* in central New England. *Ecosphere* 3, art10. <https://doi.org/10.1890/es11-0277.1>
- Palace, M., Keller, M., Asner, G.P., Hagen, S., Braswell, B., 2008. Amazon forest structure from IKONOS satellite data and the automated characterization of forest canopy properties. *Biotropica* 40, 141–150. <https://doi.org/10.1111/j.1744-7429.2007.00353.x>
- Plotkins, A.B., O’Keefe, J., Foster, D.R., 2015. Harvard University Forest, Massachusetts, United States of America, in: Siry, J.P., Bettinger, P., Merry, K., Grebner, D.L., Boston, K., Cieszewski, C. (Eds.), *Forest Plans of North America*. Elsevier Inc., pp. 69–77. <https://doi.org/10.1016/B978-0-12-799936-4.00010-2>
- Pommerening, A., 2002. Approaches to quantifying forest structures. *Forestry* 75, 305–324. <https://doi.org/10.1093/forestry/75.3.305>
- Popescu, S.C., Wynne, R.H., 2013. Seeing the Trees in the Forest. *Photogramm. Eng. Remote Sens.* 70, 589–604. <https://doi.org/10.14358/pers.70.5.589>
- Pretzsch, H., 2014. Canopy space filling and tree crown morphology in mixed-species stands compared with monocultures. *For. Ecol. Manage.* 327, 251–264. <https://doi.org/10.1016/j.foreco.2014.04.027>
- Pretzsch, H., Rais, A., 2016. Wood quality in complex forests versus even-aged monocultures: review and perspectives. *Wood Sci. Technol.* 50, 845–880. <https://doi.org/10.1007/s00226-016-0827-z>
- Pretzsch, H., Schütze, G., 2016. Effect of tree species mixing on the size structure, density, and yield of forest stands. *Eur. J. For. Res.* 135, 1–22. <https://doi.org/10.1007/s10342-015-0913-z>
- Putz, F.E., Parker, G.G., Archibald, R., 1984. Mechanical Abrasion and Intercrown Spacing. *Am. Midl. Nat.* This 112, 24–28.
- Qiao, K., Zhu, W., Xie, Z., Li, P., 2019. Estimating the Seasonal Dynamics of the Leaf Area Index Using Piecewise LAI-VI Relationships Based on Phenophases. *Remote Sens.* 11, 689. <https://doi.org/10.3390/rs11060689>
- Rainey, S.M., Nadelhoffer, K.J., Silver, W.L., Martha, R., 1999. Effects of Chronic Nitrogen Additions on Understory Species in a Red Pine Plantation. *Ecol. Appl.* 9, 949–957.
- Reich, P.B., 2014. The world-wide ‘ fast – slow ’ plant economics spectrum : a traits manifesto

275–301. <https://doi.org/10.1111/1365-2745.12211>

- Roussel, J.-R., Auty, D., 2019. lidR: Airborne LiDAR Data Manipulation and Visualization for Forestry Application.
- Rudnicki, M., Silins, U., Lieffers, V.J., Josi, G., 2001. Measure of simultaneous tree sways and estimation of crown interactions among a group of trees. *Trees - Struct. Funct.* 15, 83–90. <https://doi.org/10.1007/s004680000080>
- Rustad, L., Campbell, J., Dukes, J.S., Huntington, T., Fallon Lambert, K., Mohan, J., Rodenhouse, N., 2012. Changing climate, changing forests: The impacts of climate change on forests of the northeastern United States and eastern Canada. <https://doi.org/10.2737/NRS-GTR-99>
- Sapijanskas, J., Paquette, A., Potvin, C., Kunert, N., Loreau, M., 2012. Tropical tree diversity enhances light capture through plastic architectural changes and spatial and temporal niche differences. *Ecology* 95, 1–32. <https://doi.org/10.1890/13-1366.1>
- Shi, Y., Skidmore, A.K., Wang, T., Holzwarth, S., Heiden, U., Pinnel, N., Zhu, X., Heurich, M., 2018. Tree species classification using plant functional traits from LiDAR and hyperspectral data. *Int J Appl Earth Obs Geoinf.* 73, 207–219. <https://doi.org/10.1016/j.jag.2018.06.018>
- Silva, C.A., Hudak, A.T., Vierling, L.A., Loudermilk, E.L., O'Brien, J.J., Hiers, J.K., Jack, S.B., Gonzalez-Benecke, C., Lee, H., Falkowski, M.J., Khosravipour, A., 2016a. Imputation of Individual Longleaf Pine (*Pinus palustris* Mill.) Tree Attributes from Field and LiDAR Data. *Can. J. Remote Sens.* 42, 554–573. <https://doi.org/10.1080/07038992.2016.1196582>
- Silva, C.A., Hudak, A.T., Vierling, L.A., Loudermilk, E.L., O'Brien, J.J., Hiers, J.K., Jack, S.B., Gonzalez-Benecke, C., Lee, H., Falkowski, M.J., Khosravipour, A., 2016b. Imputation of Individual Longleaf Pine (*Pinus palustris* Mill.) Tree Attributes from Field and LiDAR Data. *Can. J. Remote Sens.* 42, 554–573. <https://doi.org/10.1080/07038992.2016.1196582>
- Small, M.J., Small, C.J., Dreyer, G.D., The, S., Society, B., Sep, N.J., Small, M.J., Small, C.J., Dreyer, G.D., 2005. Changes in a Hemlock-Dominated Forest following Woolly Adelgid Infestation in Southern New England Published by : Torrey Botanical Society Stable URL : <http://www.jstor.org/stable/20063785> Changes in a hemlock-dominated forest following woolly adelgid inf 132, 458–470.
- Stephenson, N.L., Das, A.J., Condit, R., Russo, S.E., Baker, P.J., Beckman, N.G., Coomes, D.A., Lines, E.R., Morris, W.K., Rüger, N., Álvarez, E., Blundo, C., Bunyavejchewin, S., Chuyong, G., Davies, S.J., Duque, Á., Ewango, C.N., Flores, O., Franklin, J.F., Grau, H.R., Hao, Z., Harmon, M.E., Hubbell, S.P., Kenfack, D., Lin, Y., Makana, J.R., Malizia, A., Malizia, L.R., Pabst, R.J., Pongpattananurak, N., Su, S.H., Sun, I.F., Tan, S., Thomas, D., Van Mantgem, P.J., Wang, X., Wiser, S.K., Zavala, M.A., 2014. Rate of tree carbon accumulation increases continuously with tree size. *Nature* 507, 90–93. <https://doi.org/10.1038/nature12914>
- Strigul, N., Pristinski, D., Purves, D., Dushoff, J., Pacala, S., 2008. Scaling from trees to forests : tractable macroscopic equations for forest dynamics. *Ecol. Monogr.* 78, 523–545.
- Sullivan, F.B., Ducey, M.J., Orwig, D.A., Cook, B., Palace, M.W., 2017. Forest Ecology and

- Management Comparison of lidar- and allometry-derived canopy height models in an eastern deciduous forest. *For. Ecol. Manage.* 406, 83–94. <https://doi.org/10.1016/j.foreco.2017.10.005>
- Sullivan, F.B., Ducey, M.J., Orwig, D.A., Cook, B., Palace, M.W., 2017. Comparison of lidar- and allometry-derived canopy height models in an eastern deciduous forest. *For. Ecol. Manage.* 406, 83–94. <https://doi.org/10.1016/j.foreco.2017.10.005>
- Team, Q.D., 2018. QGIS Geographic Information System.
- Team, R.C., 2018. R: A language and environment for statistical computing.
- Thompson, J.R., Carpenter, D.N., Cogbill, C. V., Foster, D.R., 2013. Four Centuries of Change in Northeastern United States Forests. *PLoS One* 8. <https://doi.org/10.1371/journal.pone.0072540>
- Valladares, F., Niinemets, U., 2007. The Architecture of Plant Crowns: From Design Rules to Light Capture and Performance. *Funct. plant Ecol.* 101–150. <https://doi.org/10.1029/2001JD001242>
- van Ewijk, K.Y., Treitz, P.M., Scott, N.A., 2013. Characterizing Forest Succession in Central Ontario using Lidar-derived Indices. *Photogramm. Eng. Remote Sens.* 77, 261–269. <https://doi.org/10.14358/pers.77.3.261>
- Vauhkonen, J., Ene, L., Gupta, S., Heinzl, J., Holmgren, J., Pitkänen, J., Solberg, S., Wang, Y., Weinacker, H., Hauglin, K.M., Lien, V., Packalén, P., Gobakken, T., Koch, B., Næsset, E., Tokola, T., Maltamo, M., 2012. Comparative testing of single-tree detection algorithms under different types of forest. *Forestry* 85, 27–40. <https://doi.org/10.1093/forestry/cpr051>
- Vincent, G., Harja, D., 2008. Exploring ecological significance of tree crown plasticity through three-dimensional modelling. *Ann. Bot.* 101, 1221–1231. <https://doi.org/10.1093/aob/mcm189>
- Vincent, L., Soille, P., 1991. Watersheds in Digital Spaces: An Efficient Algorithm Based on Immersion Simulations. *IEEE Trans. Pattern Anal. Mach. Intell.* 13, 583–598.
- Wan Mohd Jaafar, W., Woodhouse, I., Silva, C., Omar, H., Abdul Maulud, K., Hudak, A., Klauberg, C., Cardil, A., Mohan, M., 2018. Improving Individual Tree Crown Delineation and Attributes Estimation of Tropical Forests Using Airborne LiDAR Data. *Forests* 9, 759. <https://doi.org/10.3390/f9120759>
- Wang, Y., Hyyppä, J., Liang, X., Kaartinen, H., Yu, X., Lindberg, E., Holmgren, J., Qin, Y., Mallet, C., Ferraz, A., Torabzadeh, H., Morsdorf, F., Zhu, L., Liu, J., Alho, P., 2016. International Benchmarking of the Individual Tree Detection Methods for Modeling 3-D Canopy Structure for Silviculture and Forest Ecology Using Airborne Laser Scanning. *IEEE Trans. Geosci. Remote Sens.* 54, 5011–5027. <https://doi.org/10.1109/TGRS.2016.2543225>
- WARING, R.H., B.E. LAW, M.L. GOULDEN, S.L. BASSOW, R.W. McCREIGHT, S.C. WOFS, F.A. BAZZAZ, 1995. Scaling gross ecosystem production at Harvard Forest with remote sensing: a comparison of estimates from a constrained quantum-use efficiency model and eddy correlation. *Plant. Cell Environ.* 18, 1201–1213. <https://doi.org/10.1111/j.1365-3040.1995.tb00629.x>

- Williams, L.J., Paquette, A., Cavender-Bares, J., Messier, C., Reich, P.B., 2017. Spatial complementarity in tree crowns explains overyielding in species mixtures. *Nat. Ecol. Evol.* 1. <https://doi.org/10.1038/s41559-016-0063>
- Wonn, H.T., O'Hara, K.L., 2001. Height:diameter ratios and stability relationships for four northern Rocky Mountain tree species. *West. J. Appl. For.* 16, 87–94.
- Yang, J., He, Y., Caspersen, J.P., Jones, T.A., 2017. Delineating Individual Tree Crowns in an Uneven-Aged, Mixed Broadleaf Forest Using Multispectral Watershed Segmentation and Multiscale Fitting. *IEEE J. Sel. Top. Appl. Earth Obs. Remote Sens.* 10, 1390–1401. <https://doi.org/10.1109/JSTARS.2016.2638822>
- Yin, D., Wang, L., 2016. How to assess the accuracy of the individual tree-based forest inventory derived from remotely sensed data: a review. *Int. J. Remote Sens.* 37, 4521–4553. <https://doi.org/10.1080/01431161.2016.1214302>
- Zhao, Y., Zeng, Y., Zheng, Z., Dong, W., Zhao, D., Wu, B., Zhao, Q., 2018. Forest species diversity mapping using airborne LiDAR and hyperspectral data in a subtropical forest in China. *Remote Sens. Environ.* 213, 104–114. <https://doi.org/10.1016/j.rse.2018.05.014>
- Zhen, Z., Quackenbush, L.J., Stehman, S. V., Zhang, L., 2015. Agent-based region growing for individual tree crown delineation from airborne laser scanning (ALS) data. *Int. J. Remote Sens.* 36, 1965–1993. <https://doi.org/10.1080/01431161.2015.1030043>
- Zhen, Z., Quackenbush, L.J., Zhang, L., 2016. Trends in automatic individual tree crown detection and delineation-evolution of LiDAR data. *Remote Sens.* <https://doi.org/10.3390/rs8040333>